

On the Characteristics of the Conjugate Function Enabling Effective Dual Decomposition Methods

Hansi Abeynanda, Chathuranga Weeraddana, and Carlo Fischione

Abstract—We investigate a novel characteristic of the conjugate function associated to a generic convex optimization problem which can subsequently be leveraged for efficient dual decomposition methods. In particular, under mild assumptions, we show a specific region of the domain of the conjugate function where there is always a ray originating from any point of the region such that the gradients of the conjugate remain constant along the ray. We refer to this characteristic as a *fixed gradient over rays* (FGOR). We further show that the dual function inherits from the conjugate the characteristic of FGOR. Then we provide a thorough exposition of applying the FGOR characteristic to dual subgradient methods. More importantly, we leverage FGOR to devise a simple stepsize rule that can be prepended with state-of-the-art stepsize methods enabling them to be more efficient. Furthermore, we investigate how the characteristic of FGOR is used when solving the global consensus problem. We show that FGOR can be exploited not only to expedite the convergence of the dual decomposition methods but also to reduce the communication overhead when distributed implementations are sought. Numerical experiments using quadratic objectives and a regularized linear regression with a real data set are conducted to compare the practical performance of FGOR with state-of-the-art stepsize methods. Results show that the proposed approach can significantly improve the convergence of existing methods while saving a considerable amount of communication overhead.

Index Terms—Distributed optimization, conjugate function, subgradient method, dual decomposition.

I. INTRODUCTION

DISTRIBUTED algorithms for optimization problems have become necessary and pervasive in various application domains such as signal processing, machine learning, wireless communications, control systems, robotics, and many others [1]–[6]. These problems are typically of very large scale since they deal with thousands, millions, or even more variables. In this respect, effective deployment of such algorithms requires an appeal to light communication among subsystems involved in solving the optimization problem and less computational effort per subsystem, and those inevitably raise questions about how fast the deployed algorithms converge. As such, in many real-world applications, the most commonly employed method to solve optimization problems is the (sub) gradient method. The choice of (sub) gradient method sparked numerous efforts by many researchers in designing various stepsize rules and applying them to yield faster convergences [7]–[35].

H. Abeynanda and C. Fischione are with the School of Electrical Engineering and Computer Science, KTH Royal Institute of Technology, Sweden (e-mail: hkab@kth.se and carlofi@kth.se, respectively).

C. Weeraddana is with the Centre for Wireless Communication, University of Oulu, Finland (e-mail: chathuranga.weeraddana@oulu.fi).

The existing literature that designs adaptive stepsizes primarily considers subgradient methods within the primal domain. These results can be readily applied to distributed algorithms that are based on duality [36]–[39]. More specifically, in the case of dual decomposition algorithms for distributed optimization, the master problem that coordinates the subproblems at subsystems is often solved by using subgradient methods [40] where the earlier results for stepsizes can be adopted. However, these stepsize methods are applied to the dual domain without exploiting possible useful characteristics of such domain. Thus, we now pose the natural question: can we exploit any specific characteristics of the dual function itself to further scrutinize the design of stepsize rules that go beyond those designs within the primal domain for effective convergence of the subgradient method associated to the master problem?

To answer such a question, let us formalize the setting and start with the following generic primal problem:

$$\begin{aligned} & \text{minimize} && f_0(\mathbf{y}) \\ & \text{subject to} && \mathbf{y} \in \mathcal{Y} \\ & && \mathbf{A}\mathbf{y} = \mathbf{b}, \end{aligned} \quad (1)$$

where the variable is $\mathbf{y} \in \mathbb{R}^n$, $f_0 : \mathbb{R}^n \rightarrow \mathbb{R}$ is the convex objective function, $\mathbf{A} \in \mathbb{R}^{m \times n}$, $\mathbf{b} \in \mathbb{R}^m$, and \mathcal{Y} is a convex set in \mathbb{R}^n . Equivalently, one may reformulate problem (1) as

$$\begin{aligned} & \text{minimize} && f(\mathbf{y}) = f_0(\mathbf{y}) + \delta_{\mathcal{Y}}(\mathbf{y}) \\ & \text{subject to} && \mathbf{A}\mathbf{y} = \mathbf{b}, \end{aligned} \quad (2)$$

where $\delta_{\mathcal{Y}}$ denotes the indicator function of the set \mathcal{Y} , cf. Definition 2. Note that in a decomposition setting, f_0 and constraints are endowed with structural properties such as separability, enabling the application of the dual decomposition [40].

The convergence of dual decomposition methods applied to problem (2) hinges predominantly on the characteristics of the problem's associated dual function. Note that the dual function of (2) with $\mathbf{A}\mathbf{y} = \mathbf{b}$ being the constraint to which Lagrange multipliers are associated, is intimately connected with the conjugate function of f [41, § 5.1.6]. As such, to answer our posed problem, we investigate a novel characteristic of the conjugate function of f . In particular, we show that the variational geometry of \mathcal{Y} , cf. [42, Fig. 6-8] and nondifferentiable properties of f_0 induce a specific characteristic on the conjugate function. We effectively use this characteristic to devise a precursory yet simple stepsize rule that can be prepended with other stepsizes [7]–[35] while improving their convergences. The proposed precursory stepsize rule enables not only distributed but also efficient implementation of the algorithms with a light communication overhead.

A. Related Work

Employing dual decomposition techniques to solve a primal problem of the form (2) with adequate structural properties solely relies on solving the associated dual problem [40, § 2]. Recall that such a dual problem is often solved by using subgradient methods. The traditional stepsize methods [7]–[21], that have already been designed for subgradient methods are constant stepsize, line search, polynomially decay stepsizes, and geometrically decay stepsizes. These stepsizes directly apply to solving the dual problem, provided the dual function conforms to necessary regularity conditions. We give a short overview of these schemes in the following.

Given the dual function satisfies some gradient Lipschitz conditions and the Lipschitz constant is known, then a *constant stepsize* can be chosen appropriately to ensure convergence of the algorithms [7, § 1.4]. The concept of line search dates back to the 1960s [8], [9] and is used in numerous application domains [10]–[12]. It is a commonly used method for determining an appropriate stepsize, especially when the gradient Lipschitz constants are unknown. However, unlike the constant stepsize, employing line searches does not enable an effective distributed implementation of dual decomposition methods. For example, in the case of a backtracking line search, there will be an overwhelming communication overhead among subsystems even when implementing one iteration of the line search itself, *cf.* [41, p. 464].

The *polynomially decay stepsizes* such as γ_0/k and γ_0/\sqrt{k} , where $\gamma_0 > 0$ is an appropriately chosen constant [7, § 5.3], [13]–[15] are commonplace and highly popular in distributed optimization. The reason is that they can be readily applied to respective distributed algorithms because of their simple dependency on the iteration index k . Nonetheless, their drawback lies in the fact that, as they progressively decrease with each iteration, they tend to yield slow convergence [43], [44].

The *geometrically decay stepsize* strategy for subgradient methods originated from [16]–[18]. A comprehensive exposition is found in [19, § 2.3]. The resulting linear rate of convergences associated to such stepsizes has gained attention in recent studies [20], [21]. However, linear convergence is guaranteed under stringent conditions restricting the use of such stepsizes in practice [19, Theorem 2.7].

The stepsize rules considered in first-order methods [22]–[35] are different from the direct application of any traditional stepsizes discussed above. More importantly, these stepsize strategies are designed to further improve the convergences, capture more general problem formulations, and handle problems when the gradient Lipschitz constants are unknown. The rules therein can be classified as step decay stepsize [22]–[27] and running attributes-dependent stepsizes [28]–[35]. We overview them in the following.

The *step decay stepsize* is widely adopted in stochastic non-convex optimization [22]–[24] and is used as a potential model for training deep neural networks [25], [26]. This stepsize rule is characterized by maintaining constant stepsizes within stages of the algorithm iterations while decreasing it at each subsequent stage. The basic idea is to start stepping more aggressively in the initial stages and gradually become

less aggressive in subsequent stages. The rule intrinsically includes two decisions: 1) how the stepsize is reduced and 2) how the stage length is changed, over the stage count. Typically, the rule reduces the stepsize by a fixed factor at each stage, i.e., the stepsize is α^t , where $\alpha \in (0, 1)$ and t is the stage count. This policy, where the stepsize is reduced by a factor after a predetermined number of epochs, instead of at every iteration, is viewed as a variant of the geometrically decay stepsize. In contrast, the stepsize schedule employed in [24] is proportional to $1/t$, where t is the stage count. On the other hand, stage lengths are changed either with linear growth [24] or exponential growth [22] or sometimes are kept constant [23], [27]. In general, almost all step decay stepsize rules can be employed for dual decomposition methods.

The running attributes-dependent stepsizes that rely on algorithms’ runtime data, such as decision variables, gradients, and function values, are extensively studied in [28]–[35]. *Polyak’s stepsize* [28] is an appealing rule demonstrating linear convergence rates for general strongly convex functions, even under non-differentiable settings. However, it requires the optimal value of the underlying problem or initial guess of it with subsequent refinement to compute the stepsize in every iteration. Despite such restrictions, recent studies have revived interest in Polyak’s stepsize due to its linear convergence properties, *cf.* [29]–[31].

Another running attributes-dependent stepsize is the *Barzilai-Borwein (BB) rule* [32]–[34]. Unlike Polyak’s stepsize, the BB rule doesn’t require the knowledge of the optimal value of the underlying problem. Initial BB results are limited to two-dimensional quadratic objective functions with linear convergence guarantees [32]. Linear convergence with BB stepsizes under strictly convex quadratic functions, in general, has been established in [33]. Extensions of similar convergence results under more general settings, in particular, for smooth and strongly convex functions have been established in [34], however under more restricted assumptions. In [35], a more appealing stepsize is proposed without the need for any restricted assumptions like those in Polyak’s stepsize and BB rule. More specifically, the stepsize proposed in [35] requires no specific assumptions beyond the local gradient Lipschitz continuity. In a dual decomposition setting, all the above stepsize rules [28]–[35] can be deployed, given the necessary runtime data in each iteration is communicated to the entity that is updating the dual variables, e.g., a parameter server.

When solving the dual problem in a dual decomposition setting, one can always employ first-order algorithms [7]–[35] that are devised for subgradient methods. Nevertheless, it is instructive to observe that the dual function of the underlying primal formulation, can be endowed with certain characteristics to design stepsize rules to further improve the convergences. In this respect, dualization of strong convexity [42, Prop. 12.60] which entangles the gradient Lipschitzian properties of primal functions and strong convexity of the associated dual functions and vice versa is one of the most classical results that enables the choice of constant stepsize length in a dual decomposition setting, *cf.* [7, § 1.4]. But to the best of the authors’ knowledge, there seems to be no other explicit record previously of the employment of

dual characteristics towards designing stepsize rules for dual decomposition methods.

B. Our Contribution

We investigate a novel characteristic of the conjugate function associated to the convex-constrained optimization, which we can leverage to improve the performance of dual subgradient methods. In particular, within problem setting (1), the main contributions of this paper are given below.

- *Fixed-gradient-over-rays* (FGOR) characteristic of the conjugate function: we show that there is a specific region in the domain of the conjugate function f^* [cf. Definition 1] of f in problem (2) such that for all points ν in the region there is a ray originating from ν along which the gradients of f^* remain constant, cf. § II, Proposition 1.
- FGOR characteristic of the dual function: following the FGOR characteristic of f^* , we establish that the domain of the dual function g of problem (2) contains a ray along which the gradients of g remain constant, cf. § III, Corollary 1.
- Application of FGOR on the dual subgradient method: using established FGOR characteristics, we devise a simple stepsize rule that can be prepended with state-of-the-art stepsize methods while improving the convergence of the dual subgradient method, cf. § IV, Algorithm 1.
- Benefits of FGOR on the global consensus problem: we explore how the FGOR characteristics can be exploited when solving the global consensus problem [cf. (29)] using dual decomposition. In particular, we show that by utilizing FGOR characteristics, we can improve the performance of the standard dual decomposition algorithm not only in terms of the speed of the convergence but also in terms of efficient communication, cf. § V, Algorithm 3, Lemma 1, and § VI.
- Lipschitzian properties of the dual function g : under less restricted assumptions, we establish that the gradients ∇g of g are Lipschitz continuous, a more general Lipschitzian property than the existing results, cf. Appendix B, Proposition 2, Corollary 2.

C. Notation

Normal font lowercase letters x , bold font lowercase letters \mathbf{x} , bold font uppercase letters \mathbf{X} , and calligraphic font \mathcal{X} represent scalars, vectors, matrices, and sets, respectively. The set of real numbers, set of extended real numbers, set of real n -vectors, set of real $m \times n$ matrices, set of positive integers, and set of nonnegative integers are denoted by \mathbb{R} , $\overline{\mathbb{R}}$, \mathbb{R}^n , $\mathbb{R}^{m \times n}$, \mathbb{Z}_+ , and \mathbb{Z}_+^0 , respectively. The boundary of a set \mathcal{X} , the interior of a set \mathcal{X} , and the convex hull of a set \mathcal{X} are denoted by $\text{bnd } \mathcal{X}$, $\text{int } \mathcal{X}$, and $\text{con } \mathcal{X}$, respectively. The domain of a function $f : \mathbb{R}^n \rightarrow \mathbb{R}$ is a subset of \mathbb{R}^n and is denoted by $\text{dom } f$. The set of all the subgradients of a function f at a point $\mathbf{x} \in \mathbb{R}^n$ is denoted by $\partial f(\mathbf{x})$. The range of a matrix \mathbf{X} is denoted by $R(\mathbf{X})$. For a given matrix \mathbf{X} , \mathbf{X}^T denotes the matrix transpose. The positive definite cone is denoted by \mathbb{S}_{++}^n . The $n \times n$ identity matrix and the n -vectors with all entries equal to one are denoted by \mathbf{I}_n and $\mathbf{1}_n$, respectively.

D. Organization of the Paper

The rest of the paper is organized as follows. In § II, we investigate the FGOR characteristic of the conjugate function. The FGOR characteristic of the dual function is explored in § III. In § IV, the application of FGOR on the dual subgradient algorithm is discussed. Employing FGOR to solve the global consensus problem is discussed in § V. Numerical experiments are presented in § VI. Finally, we conclude the paper in § VII, followed by appendices.

II. FGOR CHARACTERISTIC OF THE CONJUGATE f^*

In this section, we demonstrate an appealing property of the conjugate function f^* of f [cf. problem (2)], that is, FGOR, which we will employ to devise our stepsize rules. Roughly speaking, we show that there is a specific region in the domain of f^* such that for all points ν in the region, there is a ray originating from ν along which the gradients of f^* remain constant. Besides, note that the dual function, g is simply a restriction of $-f^*$. As a result, further, we show that g directly inherits the FGOR characteristic from $-f^*$ if the restriction conforms to certain conditions. Then we leverage the FGOR characteristic of g to design a precursory yet simple and communication-efficient stepsize rule that can be prepended with other existing ones for improved convergences.

Let us start by making a couple of assumptions about f_0 , the set \mathcal{Y} , and the subdifferential $\partial f(\bar{\mathbf{y}})$, where $\bar{\mathbf{y}} \in \text{bnd } \mathcal{Y}$.

Assumption 1: The function f_0 is lower semicontinuous (lsc), proper, and strictly convex. The set \mathcal{Y} is convex and compact.

Note that from the practical point of view, the compact constraint set is not typically a restriction. For example, it is a common approach in many machine learning problems that impose regularization as a constraint [45], [46]. It can be shown that the problem of convex regularized minimization is equivalent to its corresponding regularization-constrained formulation [47]. Moreover, decision variables pertaining to feasible resources associated to engineering problems are usually finite [41], [48].

Assumption 2: For all $\bar{\mathbf{y}} \in \text{bnd } \mathcal{Y}$, there exists a sequence $\{\mathbf{y}_k\}_{k=1}^\infty$, $\mathbf{y}_k \in \mathcal{Y}$, with $\lim_{k \rightarrow \infty} \mathbf{y}_k = \bar{\mathbf{y}}$ such that $\limsup_{k \rightarrow \infty} \|\boldsymbol{\nu}_k\|_2 \neq \infty$ with $\boldsymbol{\nu}_k \in \partial f(\mathbf{y}_k)$.

By the assumption above, one can exclude cases of infinite gradients at the boundary of \mathcal{Y} . The function $l = l_0 + \delta_{\mathcal{Y}}$ in Example 5 [cf. Appendix B] is a case where the assumption above breaks since the gradient of the function l_0 tends to ∞ or $-\infty$ as $\bar{\mathbf{y}}$ tends to 1 or -1 , respectively.

Next, we outline a few remarks that are useful in deriving the FGOR characteristic of f^* .

Remark 1: Let

$$\mathcal{V} = \text{con } \{\partial f_0(\bar{\mathbf{y}}) \mid \bar{\mathbf{y}} \in \text{bnd } \mathcal{Y}\} \quad (3)$$

Then $\boldsymbol{\nu}_0 \in \text{int } \mathcal{V}$ if and only if $\exists \mathbf{y} \in \text{int } \mathcal{Y}$ such that $\boldsymbol{\nu}_0 \in \partial f(\mathbf{y})$.

We illustrate the set \mathcal{V} and the idea of Remark 1 using the following example for clarity.

Example 1 (An Illustration of Remark 1): Two simple functions f_1 and f_2 are considered with constraint sets \mathcal{Y}_1 and \mathcal{Y}_2 , respectively.

- 1) $f_1(\mathbf{y}) = 2\|\mathbf{y}\|_2^2 + 1$, where $\mathcal{Y}_1 = \{\mathbf{y} \in \mathbb{R}^2 \mid -[0 \ 1]^T \leq \mathbf{y} \leq [1 \ 0]^T\}$.
 2) $f_2(\mathbf{y}) = 0.5 \max\{\|\mathbf{y} - \mathbf{1}_2\|_2^2, \|\mathbf{y} + \mathbf{1}_2\|_2^2\}$, where $\mathcal{Y}_2 = \{\mathbf{y} \in \mathbb{R}^2 \mid -[2 \ 2]^T \leq \mathbf{y} \leq [2 \ 2]^T\}$.

Then $\partial f_1(\bar{\mathbf{y}})$, where $\bar{\mathbf{y}} = [\bar{y}_1 \ \bar{y}_2]^T \in \text{bnd } \mathcal{Y}_1$ is given by

$$\partial f_1(\bar{\mathbf{y}}) = \begin{cases} [4\bar{y}_1 \ 0]^T & ; \bar{y}_1 \in [0, 1], \bar{y}_2 = 0 \\ [4 \ 4\bar{y}_2]^T & ; \bar{y}_1 = 1, \bar{y}_2 \in [-1, 0] \\ [4\bar{y}_1 - 4]^T & ; \bar{y}_1 \in [0, 1], \bar{y}_2 = -1 \\ [0 \ 4\bar{y}_2]^T & ; \bar{y}_1 = 0, \bar{y}_2 \in (-1, 0). \end{cases}$$

Therefore the set \mathcal{V} associated to f_1 is given by $\mathcal{V} = \{\boldsymbol{\nu} \in \mathbb{R}^2 \mid -[0 \ 4]^T \leq \boldsymbol{\nu} \leq [4 \ 0]^T\}$, cf. Fig. 1(c). Similarly, one can show that the set \mathcal{V} associated to f_2 is given by the polyhedron with vertices $[-3 \ 3]^T$, $[-3 \ 1]^T$, $[-1 \ 3]^T$, $[3 \ 3]^T$, $[3 \ -1]^T$, and $[1 \ -3]^T$, cf. Fig. 1(d). Furthermore, to demonstrate the idea of Remark 1, consider the set \mathcal{V} associated to f_1 with $\mathbf{u} = [2 \ -2]^T$ and $\mathbf{v} = [0.5 \ -0.5]^T$. Clearly, $\mathbf{u} \in \text{int } \mathcal{V}$ and $\mathbf{u} = \nabla f_1(\mathbf{v})$, where $\mathbf{v} \in \text{int } \mathcal{V}$. Conversely, for $\mathbf{r} = [0.25 \ -0.75]^T$ and $\mathbf{s} = [1 \ -3]^T$, $\mathbf{r} \in \text{int } \mathcal{V}$ and $\mathbf{s} = \nabla f_1(\mathbf{r})$, where $\mathbf{s} \in \text{int } \mathcal{V}$.

Remark 2: Let $\bar{\mathbf{y}} \in \text{bnd } \mathcal{V}$. Then $\partial \delta_{\mathcal{Y}}(\bar{\mathbf{y}}) = N_{\mathcal{Y}}(\bar{\mathbf{y}})$, where $N_{\mathcal{Y}}(\bar{\mathbf{y}})$ denotes the normal cone of the set \mathcal{V} at $\bar{\mathbf{y}}$.

Remark 3: Let $\bar{\mathbf{y}} \in \text{bnd } \mathcal{V}$. Then $\partial f(\bar{\mathbf{y}}) = \partial f_0(\bar{\mathbf{y}}) + N_{\mathcal{Y}}(\bar{\mathbf{y}})$. Remark 3 is an immediate result due to the convexity of f_0 and $\delta_{\mathcal{Y}}$. More specifically, since $f = f_0 + \delta_{\mathcal{Y}}$ [cf. (2)] the convexity of f_0 and $\delta_{\mathcal{Y}}$ suggests that $\partial f = \partial f_0 + \partial \delta_{\mathcal{Y}}$. This together with Remark 2 yield Remark 3.

Finally, the following proposition establishes the FGOR characteristic of f^* .

Proposition 1: Suppose Assumption 1 and Assumption 2 hold. Then for all $\boldsymbol{\nu} \in \mathbb{R}^n \setminus \text{int } \mathcal{V}$, there exists $\boldsymbol{\eta} \in \mathbb{R}^n$ such that for all $\alpha \geq 0$, $\boldsymbol{\nu} + \alpha\boldsymbol{\eta} \in \mathbb{R}^n \setminus \text{int } \mathcal{V}$ and $\nabla f^*(\boldsymbol{\nu} + \alpha\boldsymbol{\eta})$ is a constant vector.

Proof: Let $\boldsymbol{\nu} \in \mathbb{R}^n \setminus \text{int } \mathcal{V}$. Then, Remark 1 confirms that $\exists \bar{\mathbf{y}} \in \text{bnd } \mathcal{V}$ such that $\boldsymbol{\nu} \in \partial f(\bar{\mathbf{y}})$, i.e.,

$$\boldsymbol{\nu} = \bar{\boldsymbol{\nu}} + \boldsymbol{\eta}, \quad (4)$$

where $\bar{\boldsymbol{\nu}} \in \partial f_0(\bar{\mathbf{y}})$ and $\boldsymbol{\eta} \in N_{\mathcal{Y}}(\bar{\mathbf{y}})$, cf. Remark 3. Now consider the ray

$$\{\boldsymbol{\nu} + \alpha\boldsymbol{\eta} \mid \alpha \geq 0\} = \{\bar{\boldsymbol{\nu}} + (1 + \alpha)\boldsymbol{\eta} \mid \alpha \geq 0\}, \quad (5)$$

where the equality follows from (4). Since $\bar{\boldsymbol{\nu}} \in \partial f_0(\bar{\mathbf{y}})$ and $\boldsymbol{\eta} \in N_{\mathcal{Y}}(\bar{\mathbf{y}})$, $\bar{\boldsymbol{\nu}} + (1 + \alpha)\boldsymbol{\eta} \in \partial f(\bar{\mathbf{y}})$ for all $\alpha \geq 0$, cf. Remark 3. Therefore, [42, Proposition 11.3], together with (5), we have

$$\nabla f^*(\boldsymbol{\nu} + \alpha\boldsymbol{\eta}) = \bar{\mathbf{y}} \quad (6)$$

for all $\alpha \geq 0$. Moreover, since $\bar{\mathbf{y}} \in \text{bnd } \mathcal{V}$, Remark 1 confirms that for all $\alpha \geq 0$, $\boldsymbol{\nu} + \alpha\boldsymbol{\eta} \in \mathbb{R}^n \setminus \text{int } \mathcal{V}$. ■

Proposition 1 indicates that for all $\boldsymbol{\nu} \in \mathbb{R}^n \setminus \text{int } \mathcal{V}$ there exists a ray $\mathcal{R}_{\boldsymbol{\nu}} = \{\boldsymbol{\nu} + \alpha\boldsymbol{\eta} \mid \alpha \geq 0\} \subseteq \mathbb{R}^n \setminus \text{int } \mathcal{V}$ that originates from $\boldsymbol{\nu}$ along which the gradients of the conjugate f^* remain constant. To illustrate this phenomenon associated to Proposition 1, we provide the following example.

Example 2 (An Illustration of Proposition 1):

Consider the functions f_1 and f_2 in Example 1. The conjugate functions f_1^* and f_2^* of $f_1 + \delta_{\mathcal{Y}_1}$ and $f_2 + \delta_{\mathcal{Y}_2}$ are depicted in Fig. 1(a) and Fig. 1(b), respectively. The level

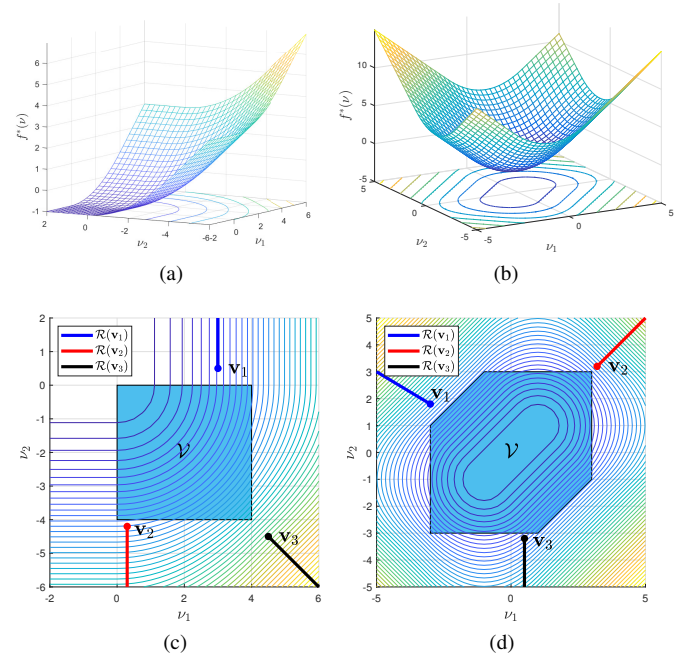


Fig. 1. An illustration of Proposition 1. (a) Conjugate function f_1^* of $f_1 + \delta_{\mathcal{Y}_1}$. (b) Conjugate function f_2^* of $f_2 + \delta_{\mathcal{Y}_2}$. (c) Level sets of f_1^* and associated set \mathcal{V} : ∇f_1^* over each ray remains intact, where $\mathcal{R}(\mathbf{v}_1)$, $\mathcal{R}(\mathbf{v}_2)$, and $\mathcal{R}(\mathbf{v}_3)$ originates at $\mathbf{v}_1 = [3 \ 0.5]^T$ extending along $\boldsymbol{\eta}_1 = [0 \ 1]^T$, $\mathbf{v}_2 = [0.3 \ -4.2]^T$ extending along $\boldsymbol{\eta}_2 = [0 \ -1]^T$, and $\mathbf{v}_3 = [4.5 \ -4.5]^T$ extending along $\boldsymbol{\eta}_3 = [1 \ -1]^T$, respectively. (d) Level sets of f_2^* and associated set \mathcal{V} : ∇f_2^* over each ray remains intact, where $\mathcal{R}(\mathbf{v}_1)$, $\mathcal{R}(\mathbf{v}_2)$, and $\mathcal{R}(\mathbf{v}_3)$ originates at $\mathbf{v}_1 = [-3 \ 1.8]^T$ extending along $\boldsymbol{\eta}_1 = [-5 \ 3]^T$, $\mathbf{v}_2 = [3.2 \ 3.2]^T$ extending along $\boldsymbol{\eta}_2 = [1 \ 1]^T$, and $\mathbf{v}_3 = [0.5 \ -3.2]^T$ extending along $\boldsymbol{\eta}_3 = [0 \ -1]^T$, respectively.

sets of the conjugate functions are shown in Fig. 1(c) and Fig. 1(d) with their corresponding sets \mathcal{V} , cf. Remark 1. The rays originated from some random points along which the gradients of the conjugate functions f_1^* and f_2^* remain constant are shown in the same plots.

III. FGOR CHARACTERISTIC OF THE DUAL FUNCTION

Let us now investigate the FGOR characteristic of the dual function g for problem (2) that is directly inherited from the conjugate function f^* , cf. § II.

Let $\boldsymbol{\lambda} \in \mathbb{R}^m$ be the Lagrange multiplier associated to the equality constraint of problem (2). Then the dual function is given by

$$\begin{aligned} g(\boldsymbol{\lambda}) &= \inf_{\mathbf{y} \in \mathbb{R}^n} (f(\mathbf{y}) - \boldsymbol{\lambda}^T(\mathbf{A}\mathbf{y} - \mathbf{b})) \\ &= - \sup_{\mathbf{y} \in \mathbb{R}^n} (\boldsymbol{\lambda}^T \mathbf{A}\mathbf{y} - f(\mathbf{y})) + \boldsymbol{\lambda}^T \mathbf{b} \\ &= -f^*(\mathbf{A}^T \boldsymbol{\lambda}) + \mathbf{b}^T \boldsymbol{\lambda}. \end{aligned} \quad (7)$$

From (7), it is clear that the dual function g is based on a restriction of $-f^*$ to a linear space. Moreover, from basic calculus rules, we have

$$\nabla g(\boldsymbol{\lambda}) = -\mathbf{A} \nabla f^*(\mathbf{A}^T \boldsymbol{\lambda}) + \mathbf{b}. \quad (8)$$

The gradient identity (8) suggests that if $\nabla f^*(\mathbf{A}^T \boldsymbol{\lambda})$ is constant for some $\mathcal{R} \subseteq R(\mathbf{A}^T)$, then so is the gradient of g , $\nabla g(\boldsymbol{\lambda})$

for all $\{\lambda \mid \mathbf{A}^T \lambda \in \mathcal{R}\}$. This is essentially the condition based on what the FGOR characteristic of g is established.

We now formalize the preceding arguments. To this end, we start by defining the collection \mathcal{A} of rays in $\mathbb{R}^n \setminus \text{int } \mathcal{V}$, where the gradients ∇f^* over each ray remain intact, *cf.* Proposition 1. In particular, for any $\nu \in \mathbb{R}^n \setminus \text{int } \mathcal{V}$, a ray originated at ν , denoted $\mathcal{R}(\nu)$ over which ∇f^* remains intact is given by

$$\mathcal{R}(\nu) = \{\nu + \alpha \eta(\nu) \mid \alpha \geq 0\}, \quad (9)$$

where $\eta(\nu) \in \mathbb{R}^n$ depends on ν , *cf.* Proposition 1. Consequently, the collection of all such rays \mathcal{A} is given by

$$\mathcal{A} = \{\mathcal{R}(\nu) \mid \nu \in \mathbb{R}^n \setminus \text{int } \mathcal{V}\}. \quad (10)$$

It is now necessary to impose the following assumption:

Assumption 3: $\exists \mathcal{R} \in \mathcal{A}$ such that $\mathcal{R} \subseteq R(\mathbf{A}^T)$.

It is worth pointing out that the above assumption holds in many problems that are important in practice, e.g., consensus problem with regularization. We defer the details to § V while outlining a toy example to demonstrate the idea.

Example 3 (An Illustration of Assumption 3): Consider minimizing the function f_2 in Example 1 with an equality constraint $\mathbf{A}\mathbf{y} = \mathbf{0}$. The corresponding optimization problem is given below.

$$\begin{aligned} & \text{minimize} && f_2(\mathbf{y}) \\ & \text{subject to} && \mathbf{y} \in \mathcal{Y}_2 \\ & && \mathbf{A}\mathbf{y} = \mathbf{0}. \end{aligned} \quad (11)$$

The sets $R(\mathbf{A}_1^T)$ and $R(\mathbf{A}_2^T)$, where $\mathbf{A}_1 = [-5 \ 3]$ and $\mathbf{A}_2 = [1 \ 1]$ are depicted in Fig.2(a). Moreover, the rays $\mathcal{R}(\mathbf{v}_1)$ and $\mathcal{R}(\mathbf{v}_2)$ [*cf.* (9)], where $\mathbf{v}_1 = [-3 \ 1.8]^T$ and $\mathbf{v}_2 = [3.2 \ 3.2]^T$, are also shown in the same figure. Clearly, $\mathcal{R}(\mathbf{v}_1) \subseteq R(\mathbf{A}_1^T)$ and $\mathcal{R}(\mathbf{v}_2) \subseteq R(\mathbf{A}_2^T)$, respectively. Thus Assumption 3 holds for problem (11).

We are now ready to show our main result about the FGOR characteristic of the dual function g , *cf.* (7).

Corollary 1: Suppose Assumption 1, Assumption 2, and Assumption 3 hold. Then $\exists \lambda \in \mathbb{R}^m$, $\exists \mu \in \mathbb{R}^m$ such that for all $\alpha \geq 0$, $\nabla g(\lambda + \alpha\mu)$ is a constant vector.

Proof: The proof is a direct consequence of Proposition 1 and Assumption 3. More specifically, from Assumption 3, there exists a ray $\mathcal{R} \in \mathcal{A}$ such that $\mathcal{R} \subseteq R(\mathbf{A}^T)$. Let $\mathcal{R} = \{\nu + \alpha\eta \mid \alpha \geq 0\}$ for some $\nu, \eta \in \mathbb{R}^n$. Now consider the inverse image $\mathcal{I}_{\mathcal{R}}$ of \mathcal{R} under the linear mapping \mathbf{A}^T . In particular, we have

$$\mathcal{I}_{\mathcal{R}} = \{\kappa \mid \mathbf{A}^T \kappa \in \mathcal{R}\} = \{\lambda + \alpha\mu \mid \alpha \geq 0\}, \quad (12)$$

where $\lambda = (\mathbf{A}\mathbf{A}^T)^{-1}\mathbf{A}\nu$ and $\mu = (\mathbf{A}\mathbf{A}^T)^{-1}\mathbf{A}\eta$, and the last equality follows from basic linear algebraic steps. Thus, from (8), together with Assumption 3, we conclude that for all $\alpha \geq 0$, $\nabla g(\lambda + \alpha\mu)$ is a constant vector. ■

We describe in the following example two instances of dual functions associated to problem (11) to demonstrate the assertions of Corollary 1.

Example 4 (An Illustration of Corollary 1): Fig. 2(b) depicts the dual functions g_1 and g_2 of problem (11) when $\mathbf{A} = \mathbf{A}_1 = [-5 \ 3]$ and $\mathbf{A} = \mathbf{A}_2 = [1 \ 1]$, respectively. The functions g_1 and g_2 are based on restrictions of $-f^*$ to $R(\mathbf{A}_1^T)$ and $R(\mathbf{A}_2^T)$,

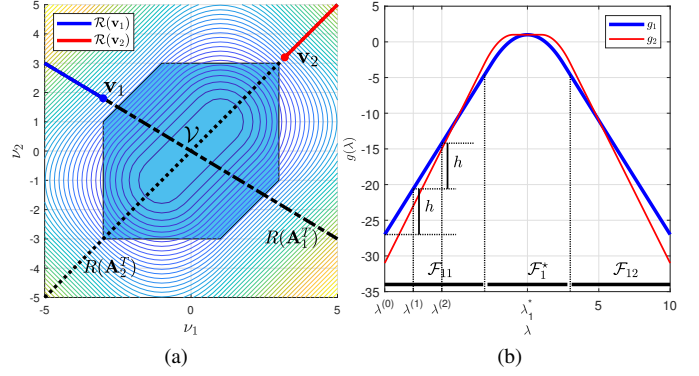


Fig. 2. An illustration of Corollary 1. (a) Level sets of f_2^* and associated set \mathcal{V} : $\mathcal{R}(\mathbf{v}_1) \subseteq R(\mathbf{A}_1^T)$ and $\mathcal{R}(\mathbf{v}_2) \subseteq R(\mathbf{A}_2^T)$. (b) Dual functions of problem (11) when $\mathbf{A} = \mathbf{A}_1$ and $\mathbf{A} = \mathbf{A}_2$: FGOR region of g_1 is $\mathcal{F}_1 = \mathcal{F}_{11} \cup \mathcal{F}_{12}$, and \mathcal{F}_1^* is the region in which the dual optimal solution $\lambda_1^* = 0$ of g_1 resides. The points $\lambda^{(0)} = -10$, $\lambda^{(1)} = -8$, and $\lambda^{(2)} = -6$ of the subgradient method (14) are due to the constant stepsizes taken in the FGOR region \mathcal{F}_{11} .

respectively, *cf.* Fig. 2(a). The figure shows both g_1 and g_2 have regions with constant gradients.

Finally, let us remark that the conjugate function and the dual function are both gradient-Lipschitz continuous. Assumption 1 is sufficient to yield such Lipschitzian properties, although we won't take this up in our subsequent stepsize designs. We note that the aforementioned Lipschitzian properties are more general than the existing results. Details are deferred to Appendix B for completeness.

In the next section, we describe how the FGOR characteristic of g [*cf.* Corollary 1] is used to devise a simple stepsize rule that can precede existing ones for improved convergences of the associated subgradient method.

IV. ON THE APPLICATION OF FGOR ON DUAL SUBGRADIENT ALGORITHM

FGOR is the prime characteristic we use in the sequel for devising our simple stepsize rule. To formalize the exposition, let us first consider the dual problem associated to problem (2):

$$\text{maximize}_{\lambda \in \mathbb{R}^m} \left(g(\lambda) = \inf_{\mathbf{y} \in \mathcal{Y}} (f_0(\mathbf{y}) - \lambda^T(\mathbf{A}\mathbf{y} - \mathbf{b})) \right). \quad (13)$$

Then the subgradient method to solve (13) is given by

$$\lambda^{(k+1)} = \lambda^{(k)} - \gamma_k \mathbf{s}^{(k)}, \quad (14)$$

where $\gamma_k > 0$ is the stepsize, $\mathbf{s}^{(k)}$ is a subgradient of $-g$ at $\lambda^{(k)} \in \mathbb{R}^m$, and k represents the iteration index.

We now give some insight into how the stepsize γ_k values should be chosen by considering problem (11) and its associated dual function g_1 depicted in Fig. 2b. The idea is very simple. Loosely speaking the stepsize rule is to use a constant stepsize as long as $\lambda^{(k)}$ is in a region of FGOR [*cf.* $\mathcal{F}_1 = \mathcal{F}_{11} \cup \mathcal{F}_{12}$, Fig. 2b], making the subgradient method yield a constant increase in the dual objective function in every iteration. For instance, moving from $\lambda^{(0)}$ to $\lambda^{(1)}$, from $\lambda^{(1)}$ to $\lambda^{(2)}$, and so forth is due to constant stepsizes since $\lambda^{(0)}, \lambda^{(1)}, \lambda^{(2)} \in \mathcal{F}_{11}$, which in turn makes the subgradient method able to have constant increments, *cf.* Fig. 2b. The

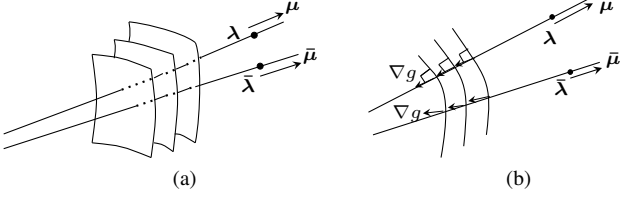


Fig. 3. An illustration of condition (15): the condition is satisfied only over the ray $\{\lambda + \alpha\mu \mid \alpha \geq 0\}$. (a) Level curves of a dual function $g : \mathbb{R}^3 \rightarrow \mathbb{R}$ and two rays with the FGOR characteristic. (b) Corresponding plan view.

important point is to make the subgradient method (14) exit the region \mathcal{F}_1 effectively and reach quickly the region \mathcal{F}_1^* in which the dual solution λ_1^* resides. As soon as the subgradient method exits the region \mathcal{F}_1 , the stepsize can be restored to any desirable existing one to guarantee convergence. Note that the constant stepsize rule we propose can precede existing ones by furnishing potential advantages as we will further explain in subsequent sections.

A. Formalizing the FGOR on Dual Subgradient

Recall from the preceding discussion that the constant stepsize rule yields a constant increase in the dual objective function in every iteration of the subgradient method (14) as long as $\lambda^{(k)}$ is in a region of FGOR. Although it is not evident in the case of the lower dimensional dual function g_1 of the preceding discussion [cf. Fig. 2b], in the context of a general formalization, an extra condition that guarantees such a constant increase of the dual function is to be considered. More specifically, among the collection of all the rays in $\text{dom } g$ with the FGOR characteristic [cf. Corollary 1], we seek for a ray $\{\lambda + \alpha\mu \mid \alpha \geq 0\}$ for which

$$\nabla g(\lambda + \alpha\mu) = -\beta\mu \quad (15)$$

for some $\beta > 0$. Fig. 3 illustrates the idea of the condition by depicting two rays $\{\lambda + \alpha\mu \mid \alpha \geq 0\}$ and $\{\tilde{\lambda} + \alpha\tilde{\mu} \mid \alpha \geq 0\}$. Note that the gradient ∇g is a constant vector over each ray. However, the condition (15) is satisfied only over the first ray.

Now it is straightforward to see that under condition (15), with constant stepsizes, the dual subgradient method (14) initialized at a point $\lambda^{(0)}$ in the ray $\{\lambda + \alpha\mu \mid \alpha \geq 0\}$ continues to remain in the same ray yielding a constant increase of the dual function g at each iteration, until $\lambda^{(k)} \notin \{\lambda + \alpha\mu \mid \alpha \geq 0\}$ for some iteration index k . When $\lambda^{(k)} \notin \{\lambda + \alpha\mu \mid \alpha \geq 0\}$, it is natural to switch to any other existing stepsize rule. More specifically, we lay out the following stepsize rule:

$$\text{If } \lambda^{(k)} \in \{\lambda + \alpha\mu \mid \alpha \geq 0\}, \text{ chose } \gamma_k = \gamma, \quad (16)$$

$$\text{Otherwise, switch to an existing stepsize rule.} \quad (17)$$

B. Determining a Ray with the FGOR Characteristic

In the case of (15), the main issue to be settled is the determination of a ray $\{\lambda + \alpha\mu \mid \alpha \geq 0\}$ over which the

condition (15) is affirmative. In this respect, the following equivalence plays an important role:

$$\begin{aligned} \nabla g(\lambda + \alpha\mu) &= -\beta\mu \\ \iff -\mathbf{A}\nabla f^*(\mathbf{A}^T(\lambda + \alpha\mu)) &= -\beta\mu - \mathbf{b} \end{aligned} \quad (18)$$

$$\iff -\mathbf{A}\nabla f^*(\nu + \alpha\eta) = -\beta(\mathbf{A}\mathbf{A}^T)^{-1}\mathbf{A}\eta - \mathbf{b}, \quad (19)$$

where (18) follows from (8), and (19) follows from that λ and μ are inverse images of some ν and η under the linear mapping \mathbf{A}^T , cf. (12). Note that $\{\nu + \alpha\eta \mid \alpha \geq 0\}$ is the image of the ray $\{\lambda + \alpha\mu \mid \alpha \geq 0\}$ under \mathbf{A}^T . The equivalence (19) confirms that a ray $\{\lambda + \alpha\mu \mid \alpha \geq 0\}$ over which condition (15) is affirmative can be determined by seeking for a ray $\mathcal{R} = \{\nu + \alpha\eta \mid \alpha \geq 0\} \in \mathcal{A}$ such that

$$\mathcal{R} \text{ conforms to (19) and} \quad (20)$$

$$\mathcal{R} \subseteq R(\mathbf{A}^T). \quad (21)$$

We start by noting that the subdifferential $\partial f(\cdot)$ evaluated at $\text{bnd } \mathcal{Y}$ [cf. Remark 3] and the collection of rays \mathcal{A} over which the gradients of the conjugate function are constant [cf. Proposition 1, (6), (10)] are intimately connected. Consequently, for fix $\bar{y} \in \text{bnd } \mathcal{Y}$, together with the inversion rule for subgradient relations [42, Prop. 11.3], we have

$$\{\nu + \alpha\eta \mid \alpha \geq 0\} \subseteq \partial f(\bar{y}) \iff \forall \alpha \geq 0, \bar{y} = \nabla f^*(\nu + \alpha\eta). \quad (22)$$

The equivalence (22) suggests that if a ray of the form $\{\nu + \alpha\eta \mid \alpha \geq 0\}$ satisfies $\bar{y} = \nabla f^*(\nu + \alpha\eta)$, then the ray resides in $\partial f(\bar{y})$. Thus, in line with this observation, together with condition (20) and condition (21), we cast the following convex feasibility problem toward yielding the ray with the intended characteristics:

$$\begin{aligned} &\text{minimize} && 0 \\ &\text{subject to} && \mathbf{A}\bar{y} - \mathbf{b} = \beta(\mathbf{A}\mathbf{A}^T)^{-1}\mathbf{A}\eta \\ & && \{\nu + \alpha\eta \mid \alpha \geq 0\} \subseteq \partial f(\bar{y}) \\ & && \{\nu + \alpha\eta \mid \alpha \geq 0\} \subseteq R(\mathbf{A}^T), \end{aligned} \quad (23)$$

where the variables are ν and η . It is straightforward to see that problem (23) can equivalently be formulated as

$$\begin{aligned} &\text{minimize} && 0 \\ &\text{subject to} && \mathbf{A}\bar{y} - \mathbf{b} = \beta(\mathbf{A}\mathbf{A}^T)^{-1}\mathbf{A}\eta \\ & && \nu \in \partial f_0(\bar{y}) + \partial \delta_{\mathcal{Y}}(\bar{y}) \\ & && \eta \in \partial \delta_{\mathcal{Y}}(\bar{y}) \\ & && \mathbf{A}^T\lambda = \nu \\ & && \mathbf{A}^T\mu = \eta, \end{aligned} \quad (24)$$

where the variables are ν , η , λ , and μ . If problem (24) is solved with solution $(\nu^*, \eta^*, \lambda^*, \mu^*)$, the ray we seek is simply given by

$$\mathcal{R}^*(\bar{y}) = \{\lambda^* + \alpha\mu^* \mid \alpha \geq 0\}. \quad (25)$$

An illustration is given in Fig. 4(a). If the problem is infeasible, one may choose a different $\bar{y} \in \text{bnd } \mathcal{Y}$.

In practice, one should have available the knowledge of $\partial f_0(\bar{y})$ to solve problem (24). It is worth noting that, in a distributed optimization setting, the global objective function f_0 is often based on local objective functions of the involved subsystems. Consequently, $\partial f_0(\bar{y})$, unlike other problem data,

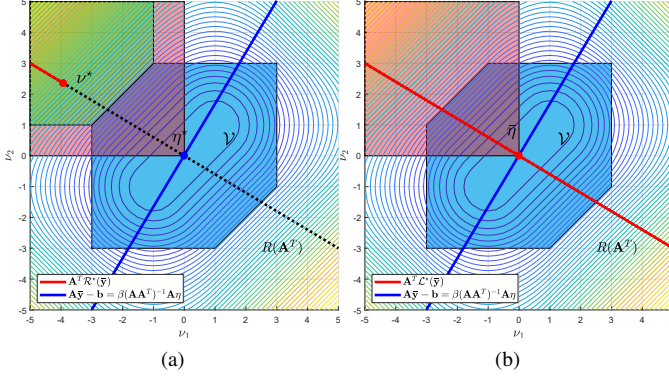


Fig. 4. An illustration of the ray $\mathcal{R}^*(\bar{\mathbf{y}})$ [cf. (25)] and the line $\mathcal{L}^*(\bar{\mathbf{y}})$ [cf. (27)] using the optimization problem (11), where $\mathbf{A} = [-0.05 \ 0.03]$, $\mathbf{b} = \mathbf{0}$, $\bar{\mathbf{y}} = [-2 \ 2]^T$, and $\beta = 1$. The sets $\partial\delta_{\mathcal{Y}_2}(\bar{\mathbf{y}})$ and $\partial f_2(\bar{\mathbf{y}}) + \partial\delta_{\mathcal{Y}_2}(\bar{\mathbf{y}})$ are depicted by the regions shaded in pink and green, respectively. (a) $\mathcal{R}^*(\bar{\mathbf{y}})$ given by solving (24): $\boldsymbol{\nu}^* = [-3.94 \ 2.36]^T$, $\boldsymbol{\eta}^* = [-0.008 \ 0.0048]^T$, $\boldsymbol{\lambda}^* = [78.72 \ 0.16]^T$, $\boldsymbol{\mu}^* = 0.16$. (b) $\mathcal{L}^*(\bar{\mathbf{y}})$ given by solving (26): $\tilde{\boldsymbol{\eta}} = [-0.008 \ 0.0048]^T$, $\tilde{\boldsymbol{\mu}} = 0.16$.

cannot be determined based on only the subsystems' local information. Therefore, this issue has to be dealt with through coordination among the subsystems. If such coordination is to be avoided, an alternative is to relax problem (24) by dropping the second constraint that entails the main coupling among subsystems. Consequently, the fourth constraint $\mathbf{A}^T \boldsymbol{\lambda} = \boldsymbol{\nu}$ becomes obsolete and the resulting relaxed formulation is given by

$$\begin{aligned} & \text{minimize} && 0 \\ & \text{subject to} && \mathbf{A}\bar{\mathbf{y}} - \mathbf{b} = \beta(\mathbf{A}\mathbf{A}^T)^{-1}\mathbf{A}\boldsymbol{\eta} \\ & && \mathbf{A}^T\boldsymbol{\mu} = \boldsymbol{\eta} \\ & && \boldsymbol{\eta} \in \partial\delta_{\mathcal{Y}}(\bar{\mathbf{y}}), \end{aligned} \quad (26)$$

where the variables are $\boldsymbol{\eta}$ and $\boldsymbol{\mu}$. A careful examination of problem (26) shows that it can be solved in two steps: 1) solve first two equations to uniquely yield the solutions $\tilde{\boldsymbol{\mu}} = (1/\beta)(\mathbf{A}\bar{\mathbf{y}} - \mathbf{b})$ and $\tilde{\boldsymbol{\eta}} = \mathbf{A}^T\tilde{\boldsymbol{\mu}}$, 2) check whether the condition $\tilde{\boldsymbol{\eta}} \in \partial\delta_{\mathcal{Y}}(\bar{\mathbf{y}})$ holds. If the condition is affirmative, then the unique solution of problem (26) is $(\tilde{\boldsymbol{\eta}}, \tilde{\boldsymbol{\mu}})$. Otherwise, a different $\bar{\mathbf{y}} \in \text{bnd } \mathcal{Y}$ may be chosen and the process is repeated.

When considering problem (26) instead of (24), there are trade-offs indeed. Unlike (24), problem (26) can be solved independently by each subsystem. This is because it is quite common in practice that the problem parameters \mathbf{A} and \mathcal{Y} of problem (1) are known by subsystems as far as distributed optimization settings are concerned (e.g., consensus problem). On the other hand, Unlike (24), the solution to problem (26) doesn't directly yield a ray as sought. Nevertheless, if feasible, we let $\tilde{\boldsymbol{\lambda}} = \tilde{\boldsymbol{\mu}}$ and consider the line given by

$$\mathcal{L}^*(\bar{\mathbf{y}}) = \{\tilde{\boldsymbol{\lambda}} + \alpha\tilde{\boldsymbol{\mu}} \mid \alpha \in \mathbb{R}\}. \quad (27)$$

It is easily seen that $\mathcal{L}^*(\bar{\mathbf{y}})$ contains a ray of the intended FGOR characteristic, cf. Fig. 4(b). This suggests the choice of the initialization point $\boldsymbol{\lambda}^{(0)}$ from $\mathcal{L}^*(\bar{\mathbf{y}})$.

Algorithm 1 Dual Subgradient Method

Require: $\Lambda(\bar{\mathbf{y}}) = \mathcal{L}^*(\bar{\mathbf{y}})$.

Require: $\boldsymbol{\lambda}^{(0)} \in \Lambda(\bar{\mathbf{y}})$.

- 1: $k = 0$.
- 2: **if** $\mathbf{A}^T \boldsymbol{\lambda}^{(k)} \in \partial f_0(\bar{\mathbf{y}}) + \partial\delta_{\mathcal{Y}}(\bar{\mathbf{y}})$ **then** \triangleright in FGOR region
- 3: Perform (14) with $\gamma_k = \gamma$ and $\mathbf{s}^{(k)} = -\boldsymbol{\mu}$.
- 4: Set $k := k + 1$ and go to step 2.
- 5: **else** \triangleright FGOR region is exited
- 6: Go to step 8. \triangleright to an existing stepsize rule
- 7: **end if**
- 8: **repeat**
- 9: Perform (14) with an existing stepsize rule.
- 10: $k := k + 1$.
- 11: **until** a stopping criterion true

C. Algorithm

We are now ready to outline the dual subgradient method with the proposed initialization and the stepsize rule that leverages FGOR characteristics. In the rest of this section, either the ray $\mathcal{R}^*(\bar{\mathbf{y}})$ [cf. (25)] or the line $\mathcal{L}^*(\bar{\mathbf{y}})$ [cf. (27)] is considered to be available. However, the algorithm is outlined with $\mathcal{L}^*(\bar{\mathbf{y}})$ for clarity¹, cf. Algorithm 1.

The condition to be checked at step 2 of Algorithm 1 is unfavorable in a distributed optimization setting. Therefore, we may wish to have at our disposal an alternative, yet equivalent representation that is favorable in a distributed setting. This is the subject of the following remark.

Remark 4: Let $\mathbf{y}^{(k)}$ be the minimizer of the Lagrangian associated to problem (2) with Lagrange multiplier $\boldsymbol{\lambda}^{(k)}$, i.e., $\mathbf{y}^{(k)} = \arg \min_{\mathbf{y} \in \mathcal{Y}} f_0(\mathbf{y}) - \boldsymbol{\lambda}^{(k)T}(\mathbf{A}\mathbf{y} - \mathbf{b})$. Then

$$\mathbf{A}^T \boldsymbol{\lambda}^{(k)} \in \partial f_0(\bar{\mathbf{y}}) + \partial\delta_{\mathcal{Y}}(\bar{\mathbf{y}}) \iff \mathbf{y}^{(k)} = \bar{\mathbf{y}} \quad (28)$$

Proof: See Appendix C. ■

In the sequel, we place a greater emphasis on the application of FGOR characteristics to the global consensus problem [49, § 7] since it is a widely used problem formulation in numerous application domains [4], [6], [50]–[52].

V. GLOBAL CONSENSUS PROBLEM

In this section, we explore how FGOR characteristics [cf. Proposition 1, Corollary 1, § IV] can be exploited when solving the global consensus problem. In particular, we consider the problem

$$\begin{aligned} & \text{minimize} && \sum_{i=1}^m f_i(\mathbf{z}) \\ & \text{subject to} && \mathbf{z} \in \mathcal{Z}, \end{aligned} \quad (29)$$

where the variable is $\mathbf{z} \in \mathbb{R}^n$. We assume that the functions $f_i : \mathbb{R}^n \rightarrow \mathbb{R}$, $i = 1, \dots, m$ and the constraint set $\mathcal{Z} \subseteq \mathbb{R}^n$ are conforming to Assumption 1 and Assumption 2. A commonly used distributed solution method for solving (29) is based on dual decomposition [40].

¹If $\mathcal{R}^*(\bar{\mathbf{y}})$ is considered, the algorithm remains the same, except that \mathcal{L}^* is replaced by \mathcal{R}^* .

Algorithm 2 Dual Decomposition Algorithm for Global Consensus Problem

Require: $\lambda \in \mathbb{R}^{n(m-1)}$.

1: $k = 0$, $\lambda^{(0)} = \lambda$. $\lambda_0^{(j)} = \lambda_m^{(j)} = \mathbf{0} \in \mathbb{R}^n$, $j \in \mathbb{Z}_+^0$.

2: Central server (CS) broadcasts $\lambda^{(0)}$ to agents.

3: **repeat**

4: $\forall i$, agent i computes:

$$\mathbf{y}_i^{(k)} = \arg \min_{\mathbf{y}_i \in \mathcal{Z}} f_i(\mathbf{y}_i) + (\lambda_i^{(k)} - \lambda_{i-1}^{(k)})^\top \mathbf{y}_i.$$

5: $\forall i$, agent i transmits $\mathbf{y}_i^{(k)}$ to CS.

6: CS computes $\mathbf{s}^{(k)} = [(\mathbf{y}_1^{(k)} - \mathbf{y}_2^{(k)})^\top \dots (\mathbf{y}_{m-1}^{(k)} - \mathbf{y}_m^{(k)})^\top]^\top$.

7: CS computes $\lambda^{(k+1)} = \lambda^{(k)} + \gamma_k \mathbf{s}^{(k)}$.

8: $\forall i$, CS broadcasts $\lambda_{i-1}^{(k+1)}$ and $\lambda_i^{(k+1)}$ to agent i .

9: $k := k + 1$.

10: **until** a stopping criterion true

A. The Standard Dual Decomposition Method

Problem (29) can be equivalently reformulated as follows:

$$\begin{aligned} & \text{minimize} && f_0(\mathbf{y}) = \sum_{i=1}^m f_i(\mathbf{y}_i) \\ & \text{subject to} && \mathbf{y}_i \in \mathcal{Z}, i \in \mathcal{S} \\ & && \mathbf{y}_i = \mathbf{y}_{i+1}, i \in \mathcal{S} \setminus \{m\}, \end{aligned} \quad (30)$$

where $\mathbf{y}_i \in \mathbb{R}^n$, $i \in \mathcal{S}$, are the local versions of \mathbf{z} , $\mathbf{y} = [\mathbf{y}_1^\top \dots \mathbf{y}_m^\top]^\top$, and $\mathcal{S} = \{1, \dots, m\}$ is the set of agents. The equality constraint $\mathbf{y}_i = \mathbf{y}_{i+1}$, $i \in \mathcal{S} \setminus \{m\}$ is introduced to impose the consistency among the local variables \mathbf{y}_i s. Then the dual function $g : \mathbb{R}^{n(m-1)} \rightarrow \overline{\mathbb{R}}$ of problem (30) is given by

$$g(\lambda) = \inf_{\mathbf{y}_i \in \mathcal{Z}, i \in \mathcal{S}} \left[\sum_{i=1}^m f_i(\mathbf{y}_i) + \sum_{i=1}^{m-1} \lambda_i^\top (\mathbf{y}_i - \mathbf{y}_{i+1}) \right], \quad (31)$$

where $\lambda_i \in \mathbb{R}^n$ denotes the Lagrange multiplier associated to the constraint $\mathbf{y}_i = \mathbf{y}_{i+1}$, $i \in \mathcal{S} \setminus \{m\}$ and $\lambda = [\lambda_1^\top \dots \lambda_{m-1}^\top]^\top$. Moreover, the dual problem associated to (30) is given by

$$\text{maximize}_{\lambda \in \mathbb{R}^{n(m-1)}} g(\lambda). \quad (32)$$

The standard dual decomposition algorithm for solving (32) is given by Algorithm 2.

In Algorithm 2, CS performs the dual variable update [cf. step 7] using any standard stepsize rule [7]–[35]. It is worth noting that when the FGOR characteristic of g is utilized, the communication steps 5 and 8 in Algorithm 2 are not needed as long as $\lambda^{(k)}$ resides in a FGOR region. In particular, utilizing the FGOR characteristic of g , we can improve the performance of Algorithm 2 not only in terms of the speed of the convergence but also in terms of communication efficiency. We discuss this idea more formally in the following subsection.

B. Using the FGOR Characteristic of g on Algorithm 2

For our exposition of using the FGOR characteristic of g on Algorithm 2, we start by noting that the constraints $\mathbf{y}_i \in \mathcal{Z}$, $i \in \mathcal{S}$ and $\mathbf{y}_i = \mathbf{y}_{i+1}$, $i \in \mathcal{S} \setminus \{m\}$ are equivalent with $\mathbf{y} \in \mathcal{Z}^m$ and $\mathbf{A}\mathbf{y} = \mathbf{0}$, respectively, where $\mathbf{y} = [\mathbf{y}_1^\top \dots \mathbf{y}_m^\top]^\top$

Algorithm 3 Dual Decomposition Algorithm with FGOR

Require: $\Lambda(\bar{\mathbf{y}}) = \mathcal{L}^*(\bar{\mathbf{y}})$.

Require: $\lambda^{(0)} \in \Lambda(\bar{\mathbf{y}})$.

1: $k = 0$.

2: $\forall i$, agent i computes:

$$\mathbf{y}_i^{(k)} = \arg \min_{\mathbf{y}_i \in \mathcal{Z}} f_i(\mathbf{y}_i) + (\lambda_i^{(k)} - \lambda_{i-1}^{(k)})^\top \mathbf{y}_i.$$

3: $\forall i$, agent i transmits CS one-bit information b_i , where

$$b_i = \begin{cases} 0; & \mathbf{y}_i^{(k)} = \bar{\mathbf{y}}_i \\ 1; & \text{Otherwise.} \end{cases} \quad (34)$$

4: CS computes $\bar{b} = \max_{i \in \mathcal{S}} b_i$.

5: $\forall i$, CS broadcasts \bar{b} to agent i .

6: **if** $\bar{b} = 0$, **then** ▷ in FGOR region

7: $\forall i$, agent i and CS perform (14) with

$$\gamma_k = \gamma \text{ and } \mathbf{s}^{(k)} = -\tilde{\boldsymbol{\mu}}.$$

8: Set $k := k + 1$ and go to step 2.

9: **else** ▷ FGOR region is exited

10: Go to step 12.

11: **end if**

12: $\forall i$, agent i transmits $\mathbf{y}_i^{(k)}$ to CS.

13: CS performs (14) using γ_k in Algorithm 2, where

$$\mathbf{s}^{(k)} = [(\mathbf{y}_1^{(k)} - \mathbf{y}_2^{(k)})^\top \dots (\mathbf{y}_{m-1}^{(k)} - \mathbf{y}_m^{(k)})^\top]^\top.$$

14: Switch to Algorithm 2 with $\lambda = \lambda^{(k+1)}$.

and \mathcal{Z}^m is the m -fold Cartesian product of \mathcal{Z} . The matrix $\mathbf{A} \in \mathbb{R}^{n(m-1) \times nm}$ has the form

$$\mathbf{A} = \begin{bmatrix} \mathbf{I}_n & -\mathbf{I}_n & \mathbf{0} & \dots & \mathbf{0} \\ \mathbf{0} & \mathbf{I}_n & -\mathbf{I}_n & \ddots & \vdots \\ \vdots & \ddots & \ddots & \ddots & \mathbf{0} \\ \mathbf{0} & \dots & \mathbf{0} & \mathbf{I}_n & -\mathbf{I}_n \end{bmatrix}. \quad (33)$$

We let $\mathcal{Z}^m = \mathcal{Y}$ for clarity. Suppose that the feasibility problem (26) associated to problem (30) is feasible for some $\bar{\mathbf{y}} = [\bar{\mathbf{y}}_1^\top \dots \bar{\mathbf{y}}_m^\top]^\top \in \text{bnd } \mathcal{Y}$, where $\bar{\mathbf{y}}_i \in \mathcal{Z}$, $\forall i \in \mathcal{S}$. Then Algorithm 3 outlines how the FGOR characteristic of the dual function g is leveraged to solve problem (30) using dual decomposition. Note that Algorithm 3 is a blend of Algorithm 1 [cf. § IV] and Algorithm 2 in the sense that we exploit the steps described in Algorithm 1 to leverage FGOR characteristics on Algorithm 2. In particular, steps 2-6 of Algorithm 3 are corresponding to step 2 of Algorithm 1, where step 6 is the criterion we set in Algorithm 3 to check whether $\lambda^{(k)}$ is in a FGOR region. Roughly speaking, if $\bar{b} = 0$, it is straightforward to see that $\mathbf{y}^{(k)} = \bar{\mathbf{y}}$ [cf. (34)], and thus $\lambda^{(k)}$ is in a FGOR region, cf. Remark 4. Moreover, steps 3-4 and steps 5-11 of Algorithm 1 are corresponding to steps 7-8 and steps 9-14 of Algorithm 3, respectively.

A natural selection for $\lambda^{(0)}$ in Algorithm 3 is $\lambda^{(0)} = \tilde{\boldsymbol{\mu}}$, cf. 27. It is worth noting that each agent i and the CS can individually solve (26). If feasible, the solutions $\tilde{\boldsymbol{\eta}}$ and $\tilde{\boldsymbol{\mu}}$ obtained by solving (26) are the same for all agents and

CS. Thus, both CS and each agent i know $\lambda^{(0)}$ and the dual subgradient is $s^{(k)} = -\tilde{\mu}$ as long as $\lambda^{(k)}$ resides in the respective FGOR region, *cf.* steps 6-7. This enables each agent i to perform the dual variable update (14) individually and in parallel until $\lambda^{(k)}$ exits the FGOR region, *cf.* step 9. However, the CS also performs the same computation to keep track of the update $\lambda^{(k)}$ to use it after the algorithm steps exit the FGOR region, *cf.* steps 13-14. We discuss the efficiency of Algorithm 3 compared to Algorithm 2 in the sequel in detail.

1) *Fast Convergence with FGOR*: Rather than choosing $\lambda^{(0)}$ arbitrarily as in Algorithm 2, Algorithm 3 is initialized with $\lambda^{(0)}$ by exploiting the FGOR characteristic of the dual function g , *cf.* problem (26). Unlike Algorithm 2, $\lambda^{(0)}$ in Algorithm 3 permits one to use fixed stepsizes and makes the subgradient algorithm [*cf.* (14)] evolve along the specified ray yielding constant increments of g as long as $\lambda^{(k)}$ resides in a FGOR region. Intuitively speaking, such a choice is fast in the sense that it directly drives $\lambda^{(k)}$ toward λ^* instead of potential detours where diminishing stepsizes such as $\gamma_0/k, \gamma_0/\sqrt{k}$ can be ineffective. Our choice of $\lambda^{(0)}$ for Algorithm 3 can also be considered as a warm-start initialization that expedites the convergence of the algorithm toward the intended solution.

2) *Efficient Communication with FGOR*: Note that Algorithm 2 requires each agent i to transmit n real numbers, i.e., $\mathbf{y}_i^{(k)} \in \mathbb{R}^n$ in step 5. In addition, it also requires CS to broadcast $n(m-1)$ real numbers to agents, *cf.* step 8. Therefore, if b bits are used to represent each real number, then Algorithm 2 requires $mnb + n(m-1)b = nb(2m-1)$ bits per epoch². However, at the corresponding steps of Algorithm 3 [*cf.* step 3 and step 5], only *one-bit* communication is needed and it does not depend on the length n of $\mathbf{y}_i^{(k)}$. More specifically, in each epoch, Algorithm 3 requires only $m+1$ bits, i.e., m bits at step 3 and one bit at step 5, as long as $\lambda^{(k)}$ resides in a region of FGOR. It is worth noting that engineering problems in real-world applications can consist of decision variables whose size n can be in the order of several thousands, or even more [53]. Thus, by leveraging FGOR characteristics, Algorithm 3 can yield a considerable reduction in the communication overhead.

C. Problem (30) with ℓ_∞ -norm Constraints

In this section, we exploit specific structural properties of the constraint set \mathcal{Z} in the consensus problem (29) to yield feasible $\bar{\mathbf{y}} \in \mathcal{Y}$ for the feasibility problem (26), where $\mathcal{Y} = \mathcal{Z}^m$. In particular, when \mathcal{Z} conforms to ℓ_∞ -norm constraints³, we show that problem (26) associated to (30) is feasible for some particular $\bar{\mathbf{y}} \in \mathcal{Y}$. We first lay out the following remark which will be useful in the sequel for our exposition.

Remark 5: Let $\mathcal{X} = \{\mathbf{x} \in \mathbb{R}^n \mid \|\mathbf{x}\|_\infty \leq c\}$, where $c \in \mathbb{R}$. Moreover, let \mathcal{V} be the set of all vertices of \mathcal{X} and $\bar{\mathbf{x}} = [x_1 \dots x_n]^T \in \mathcal{V}$, where $\forall i = 1, \dots, n, x_i \in \mathbb{R}$. Then

$$N_{\mathcal{X}}(\bar{\mathbf{x}}) = \{\mathbf{p} = [p_1 \dots p_n]^T \mid \forall i p_i \in \mathbb{R}, p_i \leq 0 \text{ if } x_i \leq 0\}. \quad (35)$$

²In the case of 64-bit double precision floating point number format $b = 64$.

³Typically, ℓ_∞ -norm constraints appear in machine learning applications. For example, the ℓ_∞ regularization can be considered as a form of constraint on the ℓ_∞ norm of parameters.

Then the following lemma substantiates the feasibility of problem (26) associated to problem (30).

Lemma 1: Let Assumption 1 and Assumption 2 hold. Suppose $\mathcal{Z} = \{\mathbf{z} \in \mathbb{R}^n \mid \|\mathbf{z}\|_\infty \leq a\}$, where $a \in \mathbb{R}$. Let $\bar{\mathbf{y}} = [\bar{\mathbf{y}}_1^T \dots \bar{\mathbf{y}}_m^T]^T \in \text{bnd } \mathcal{Z}^m$, where $\forall i \in \mathcal{S}$,

$$\bar{\mathbf{y}}_i = \begin{cases} a\mathbf{1}_n & ; \quad i \text{ odd} \\ -a\mathbf{1}_n & ; \quad i \text{ even.} \end{cases} \quad (36)$$

Then problem (26) associated to problem (30) is feasible.

Proof: It is straightforward to see that the unique solutions to the feasibility problem (26) associated to problem (30) are given by $\tilde{\mu} = (1/\beta)\mathbf{A}\bar{\mathbf{y}}$ and $\tilde{\eta} = \mathbf{A}^T\tilde{\mu}$. Thus, with our choice of $\bar{\mathbf{y}}$, we have

$$\tilde{\mu} = (1/\beta)[2a\mathbf{1}_n^T \quad -2a\mathbf{1}_n^T \quad 2a\mathbf{1}_n^T \quad \dots]^T \in \mathbb{R}^{n(m-1)}, \quad (37)$$

$$\text{and } \tilde{\eta} = \begin{cases} (1/\beta)[2a\mathbf{1}_n^T \quad -2a\mathbf{1}_n^T]^T; & m = 2 \\ (1/\beta)[2a\mathbf{1}_n^T \quad -4a\mathbf{1}_n^T \quad 4a\mathbf{1}_n^T \quad -4a\mathbf{1}_n^T \quad \dots \quad 2a\mathbf{1}_n^T]^T; & m \text{ odd, } m \geq 3 \\ (1/\beta)[2a\mathbf{1}_n^T \quad -4a\mathbf{1}_n^T \quad 4a\mathbf{1}_n^T \quad -4a\mathbf{1}_n^T \quad \dots \quad -2a\mathbf{1}_n^T]^T; & m \text{ even, } m \geq 4. \end{cases} \quad (38)$$

Clearly, $\tilde{\eta} \in N_{\mathcal{Y}}(\bar{\mathbf{y}})$, where $\mathcal{Y} = \mathcal{Z}^m$, *cf.* Remark 5. Thus $\tilde{\eta} \in \partial\delta_{\mathcal{Y}}(\bar{\mathbf{y}})$, *cf.* Remark 2. Hence problem (26) is feasible. ■

Lemma 1 indicates that problem (26) associated to problem (30) is feasible if we select $\bar{\mathbf{y}}$ according to (36), and the unique solution $(\tilde{\eta}, \tilde{\mu})$ can be derived. Thus, as we have already pointed out in Section V-B, we can choose $\lambda^{(0)} = \tilde{\mu}$ for some $\beta \in \mathbb{R}$ [*cf.* (37)] as an initialization point of Algorithm 3. In the sequel, we numerically evaluate the performance of Algorithm 3 with this choice of initialization point.

VI. NUMERICAL RESULTS

In this section, we numerically evaluate the benefits of FGOR characteristics for solving the global consensus problem (29), *cf.* § V. In particular, we compare the performance of Algorithm 3 against Algorithm 2. The comparisons are demonstrated with the following stepsize rules: 1) traditional stepsizes: constant stepsize $\gamma_k = \gamma_0$, polynomially decay stepsizes $\gamma_k = \gamma_0/k, \gamma_0/\sqrt{k}$, and geometrically decay stepsize $\gamma_k = \gamma_0q^k$, where $\gamma_0 > 0$ is an appropriately chosen constant, 2) step decay stepsize [23], 3) stepsize rule [35]. Moreover, the results are illustrated under two cases, CASE 1: the local functions f_i s in the distributed consensus formulation (30) are quadratic, and CASE 2: problem (30) is the regularized least squares regression with a real data set. For each case, we conduct experiments for $\mathbf{y}^* \in \text{int } \mathcal{Y}$ and $\mathbf{y}^* \in \text{bnd } \mathcal{Y}$, where $\mathcal{Y} = \mathcal{Z}^m$ and \mathcal{Z} is an ℓ_∞ -norm constraint, *cf.* Lemma 1. For Algorithm 3, we choose $\lambda^{(0)} = \tilde{\mu}$ for some $\beta \in \mathbb{R}$, *cf.* (37). Furthermore, the constant stepsize γ of Algorithm 3 [*cf.* step 7] is chosen to be sufficiently small to avoid undesired stepping over the region \mathcal{V} , *cf.* (3). Note that the initialization point $\tilde{\mu}$ of Algorithm 3 is deterministic and is computed in advance, *cf.* problem (26), (37). However, since the initialization for Algorithm 2 is arbitrary, for a fair comparison, an average performance of the algorithm is considered. More specifically

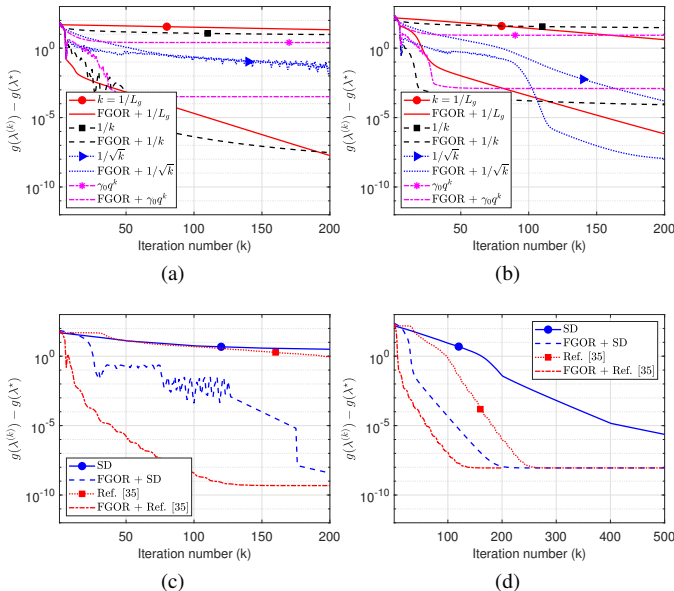


Fig. 5. CASE 1: $\mathbf{y}^* \in \text{int } \mathcal{Y}$: Comparison of results with traditional stepsizes, step decay stepsize (SD), and Ref. [35]. (a) Traditional stepsizes: $m = 4$ and $n = 3$. (b) Traditional stepsizes: $m = 4$ and $n = 10$. (c) SD and Ref. [35]: $m = 4$ and $n = 3$. (d) SD and Ref. [35]: $m = 4$ and $n = 10$.

the initialization point $\lambda^{(0)}$ of Algorithm 2 is chosen uniformly over the sphere centered at λ^* with radius $\|\bar{\mu} - \lambda^*\|_2$.

A. Case 1: Experiments with Quadratic Local Objectives

We consider problem (30) with quadratic f_i s, i.e., $f_i(\mathbf{y}_i) = \mathbf{y}_i^T \mathbf{A}_i \mathbf{y}_i + \mathbf{q}_i^T \mathbf{y}_i$, $i \in \mathcal{S}$, where $\mathbf{A}_i \in \mathbb{S}_{++}^n$ and $\mathbf{q}_i \in \mathbb{R}^n$ are arbitrarily chosen.

Fig. 5 and Fig. 6 show the comparison of results when $\mathbf{y}^* \in \text{int } \mathcal{Y}$ and $\mathbf{y}^* \in \text{bnd } \mathcal{Y}$, respectively. In particular, Fig. 5 shows the convergence of dual function values using $m = 4$ agents when the lengths of \mathbf{y}_i s are $n = 3$ and $n = 10$. Fig. 6 captures the corresponding convergences with $m = 3$ and $m = 5$ using scalar-valued \mathbf{y}_i s. For the constant stepsize rule, we choose $\gamma_k = 1/L_g$, where L_g represents the gradient Lipschitz constant of g . Both figures show that Algorithm 3 achieves significantly faster convergences than Algorithm 2. To further clarify, the comparison of results in Fig. 5(d) is summarized in Table I. For each method, the number of iterations and the total number of bits required to achieve an accuracy of 10^{-5} are given by k^* and b^* , respectively. Furthermore, for our method $b^* = k_0(m+1) + n(k^* - k_0)(2m-1)b$ and for the other methods $b^* = nk^*(2m-1)b$, where k_0 is the number of iterations that $\lambda^{(k)}$ lies in the FGOR region and b is the bits used to represent each component of communicated vectors $\mathbf{y}_i^{(k)}$ and $\lambda_i^{(k)}$, cf. § V-B2.

B. Case 2: Regularized Least Squares Regression

We consider problem (30) to be the least squares regression with ℓ_∞ -norm regularization. Then the corresponding regularized problem has the form

$$\begin{aligned} & \text{minimize} && f_0(\mathbf{y}) = \sum_{i=1}^m f_i(\mathbf{y}_i) + d\|\mathbf{y}\|_\infty^2 \\ & \text{subject to} && \mathbf{y} \in \mathcal{Y} \\ & && \mathbf{A}\mathbf{y} = \mathbf{0}, \end{aligned} \quad (39)$$

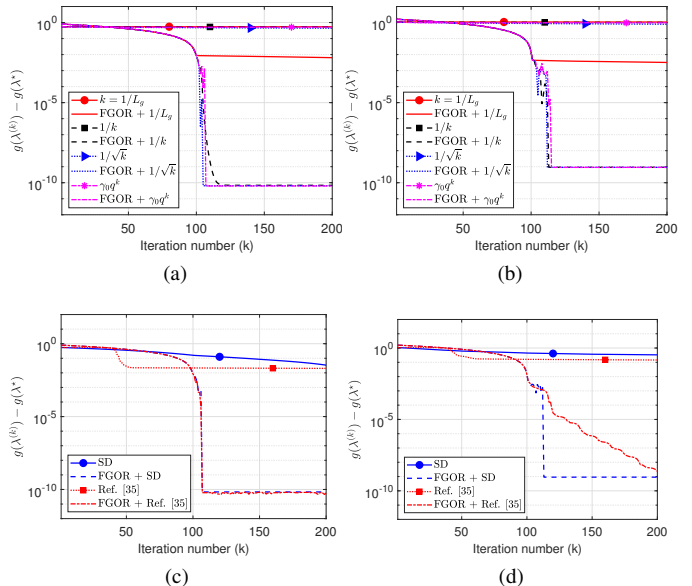


Fig. 6. CASE 1: $\mathbf{y}^* \in \text{bnd } \mathcal{Y}$: Comparison of results with traditional stepsizes, step decay stepsize (SD), and Ref. [35]. (a) Traditional stepsizes: $m = 3$ and $n = 1$. (b) Traditional stepsizes: $m = 5$ and $n = 1$. (c) SD and Ref. [35]: $m = 3$ and $n = 1$. (d) SD and Ref. [35]: $m = 5$ and $n = 1$.

where $\mathbf{y} = [\mathbf{y}_1^T \dots \mathbf{y}_m^T]^T$, $\mathcal{Y} = \mathcal{Z}^m$, \mathbf{A} is given in (33), and $d > 0$ is the regularization parameter. As we have already pointed out in Assumption 1 [cf. § II], the problem of convex regularized minimization is equivalent to its corresponding regularization-constrained formulation [47, § 1.2]. Thus, problem (39) can be equivalently reformulated as

$$\begin{aligned} & \text{minimize} && f_0(\mathbf{y}) = \sum_{i=1}^m f_i(\mathbf{y}_i) \\ & \text{subject to} && \|\mathbf{y}\|_\infty^2 \leq \bar{d} \\ & && \mathbf{A}\mathbf{y} = \mathbf{0}, \end{aligned} \quad (40)$$

where $\bar{d} > 0$ is a hyperparameter. We consider each f_i , $i \in \mathcal{S}$, in (40) with form

$$f_i(\mathbf{y}_i) = \frac{1}{N}(\mathbf{y}_i^T \mathbf{x}_i - t_i)^2, \quad (41)$$

where $\mathbf{x}_i \in \mathbb{R}^n$ is the feature vector, t_i is the observation, and N is the number of training examples of agent i . We have performed the experiments with the real estate valuation dataset [54] which contains 276 training data samples and 138 testing data samples. The length of the feature vector \mathbf{x}_i is $n = 6$. Since the features have different units, the data set is standardized before we run the experiments.

Fig. 7 and Fig. 8 show the comparison of results when $\mathbf{y}^* \in \text{int } \mathcal{Y}$ and $\mathbf{y}^* \in \text{bnd } \mathcal{Y}$, respectively. Both figures show the convergence of dual function values with $m = 3$ and $m = 6$, that is, each agent having $N_1 = 46$ and $N_2 = 96$ data samples, respectively. Similarly to CASE 1, both figures show that Algorithm 3 converges towards the optimal solution much faster than Algorithm 2. A summary of results similar to Fig. 5(d) is also provided in Table I for Fig. 8(d).

VII. CONCLUSION

A novel characteristic of the conjugate function associated to a generic convex optimization problem was investigated,

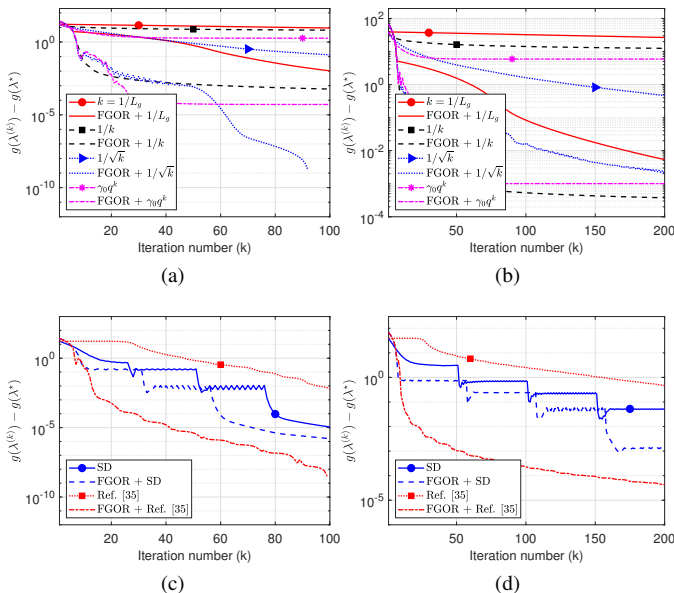


Fig. 7. CASE 2: $\mathbf{y}^* \in \text{int } \mathcal{Y}$: Comparison of results with traditional stepsizes, step decay stepsize (SD), and Ref. [35]. (a) Traditional stepsizes: $m = 3$. (b) Traditional stepsizes: $m = 6$. (c) SD and Ref. [35]: $m = 3$. (d) SD and Ref. [35]: $m = 6$.

which is referred to as FGOR. Based on this characterization, we have also established the FGOR characteristic of the associated dual function. This characteristic, in turn, is used to devise a simple stepsize policy for dual subgradient methods that can be prepended with state-of-the-art stepsize rules enabling faster convergences. Moreover, we have explored how the FGOR characteristics can be exploited when solving the global consensus problem using dual decomposition. More importantly, we have shown that FGOR can be leveraged to improve the performance of the dual decomposition methods not only in terms of the speed of convergence but also in terms of communication efficiency. Numerical experiments were conducted to evaluate the performance of the dual decomposition methods by exploiting the FGOR characteristics. Results showed that FGOR together with the devised stepsize rule can significantly improve the convergence of dual decomposition methods while reducing the considerable amount of communication overhead. As such, our theoretical and empirical expositions suggested the importance of exploiting the structure of the problem, especially for large-scale problems that are common in almost all engineering application domains, such as signal processing and machine learning.

APPENDIX A DEFINITIONS

Definition 1 (Conjugate Function): Let $f : \mathbb{R}^n \rightarrow \overline{\mathbb{R}}$. Then the function $f^* : \mathbb{R}^n \rightarrow \overline{\mathbb{R}}$ defined by $f^*(\mathbf{y}) = \sup_{\mathbf{x} \in \text{dom } f} (\mathbf{y}^T \mathbf{x} - f(\mathbf{x}))$ is called the conjugate of f .

Definition 2 (Indicator Function): Let $\mathcal{C} \subseteq \mathbb{R}^n$. Then the function $\delta_{\mathcal{C}}$ defined by $\delta_{\mathcal{C}}(\mathbf{x}) = 0$ if $\mathbf{x} \in \mathcal{C}$, and $\delta_{\mathcal{C}}(\mathbf{x}) = \infty$ if $\mathbf{x} \notin \mathcal{C}$ is called the indicator function of the set \mathcal{C} .

Definition 3 (Lipschitz Continuity): Let $f : \mathbb{R}^n \rightarrow \mathbb{R}$ with $\text{dom } f = \mathcal{X}$. Then f is Lipschitz continuous on $\mathcal{C} \subseteq \mathcal{X}$, if

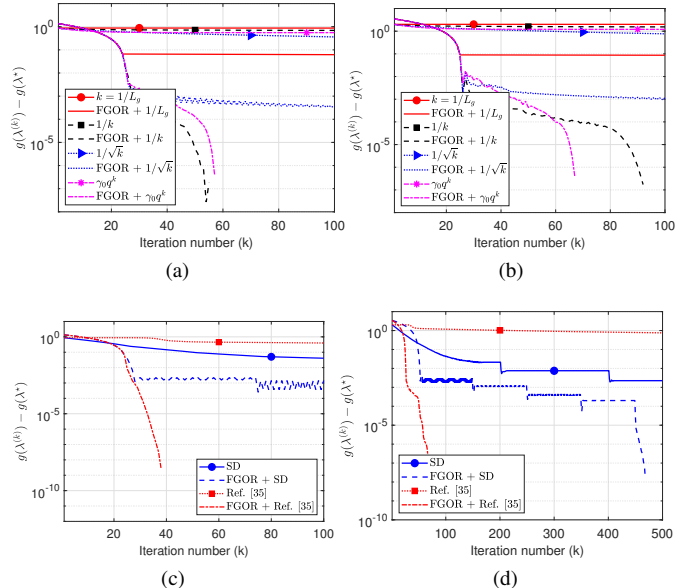


Fig. 8. CASE 2: $\mathbf{y}^* \in \text{bnd } \mathcal{Y}$: Comparison of results with traditional stepsizes, step decay stepsize (SD), and Ref. [35]. (a) Traditional stepsizes: $m = 3$. (b) Traditional stepsizes: $m = 6$. (c) SD and Ref. [35]: $m = 3$. (d) SD and Ref. [35]: $m = 6$.

$\exists L \geq 0$, s.t. $\|f(\mathbf{x}) - f(\mathbf{y})\|_2 \leq L\|\mathbf{x} - \mathbf{y}\|_2$, $\forall \mathbf{x}, \mathbf{y} \in \mathcal{C}$, where L is called the Lipschitz constant for f on \mathcal{C} .

Definition 4 (Strong Convexity): Let $f : \mathbb{R}^n \rightarrow \mathbb{R}$ with $\text{dom } f = \mathcal{X}$. Then f is strongly convex on $\mathcal{C} \subseteq \mathcal{X}$, if $\exists l > 0$, s.t. $f(t\mathbf{x} + (1-t)\mathbf{y}) \leq tf(\mathbf{x}) + (1-t)f(\mathbf{y}) - \frac{1}{2}lt(1-t)\|\mathbf{x} - \mathbf{y}\|_2^2$, $\forall \mathbf{x}, \mathbf{y} \in \mathcal{C}$, when $0 < t < 1$, where l is called the strong convexity constant for f on \mathcal{C} .

Definition 5 (Relative Interior of a Convex Set): The relative interior of a convex set \mathcal{X} relative to its affine hull is called the relative interior of \mathcal{X} , and is denoted by $\text{rint } \mathcal{X}$.

APPENDIX B LIPSCHITZIAN PROPERTIES OF f^* AND g

We derive Lipschitzian properties of the conjugate function f^* of f [cf. (2)] and the dual function g of problem (2) under Assumption 1. Since we consider strictly convex functions, our results are more general than the existing Lipschitzian properties for strongly convex objective functions [42, Prop. 12.60]. We first outline some results that are useful when asserting the intended results.

Lemma 2: Suppose Assumption 1 holds. Then the conjugate function f^* of f is lsc, proper, and strictly convex with $\text{dom } f^* = \mathbb{R}^n$.

Proof: The result follows directly from Theorem 11.1 of [42], together with that $f^*(\boldsymbol{\nu})$ is finite for all $\boldsymbol{\nu} \in \mathbb{R}^n$. ■

Lemma 3: Suppose Assumption 1 holds. Then the conjugate function f^* of f is differentiable on \mathbb{R}^n .

Proof: Since Assumption 1 holds, the function f is almost strictly convex, in the sense that f is strictly convex in $\text{rint } \mathcal{Y}$, cf. Definition 5. Thus, Theorem 11.13 of [42] guarantees that f^* is almost differentiable on $\text{int}(\text{dom } f^*) = \mathbb{R}^n$ [cf. Lemma 2], which in turn guarantees that f^* is differentiable on \mathbb{R}^n . ■

TABLE I
SUMMARY OF RESULTS IN FIG. 5(D) AND FIG. 8(D)

Figure	Method	k^*	k_0	b^*
Fig. 5(d)	FGOR + SD	115	21	105 + 6580b
	SD	421	NA	29470b
	FGOR + Ref [35]	61	5	25 + 3920b
	Ref [35]	183	NA	12810b
Fig. 8(d)	FGOR + SD	451	49	343 + 30954b
	SD	> 1000 ^a	NA	> 77000b
	FGOR + Ref [35]	57	25	175 + 2464b
	Ref [35]	$\gg 1000$ ^b	NA	$\gg 77000b$

^a For $k = 1000$ iterations, $g(\lambda^{(k)}) - g(\lambda^*) = 5.4471 \times 10^{-4}$.

^b For $k = 1000$ iterations, $g(\lambda^{(k)}) - g(\lambda^*) = 0.524$.

Lemma 4: Suppose Assumption 1 holds. Then the gradient ∇f^* of the conjugate function f^* is bounded. In particular,

$$\|\nabla f^*(\nu)\|_2 \leq \max_{y \in \mathcal{Y}} \|y\|_2 \quad \forall \nu. \quad (42)$$

Proof: Proposition 11.3 of [42], together with Assumption 1 and Lemma 3 ensures that

$$\bar{\nu} \in \partial f(\bar{y}) \iff \bar{y} \in \partial f^*(\bar{\nu}) \iff \bar{y} \in \{\nabla f^*(\bar{\nu})\}.$$

Thus, $\bar{y} = \nabla f^*(\bar{\nu})$. The result follows immediately by using that $\bar{y} \in \mathcal{Y}$. ■

Next, the following proposition claims the Lipschitzian property of the conjugate function f^* of f .

Proposition 2: Suppose Assumption 1 holds. Then the gradient ∇f^* of f^* is Lipschitz continuous with the constant $L = \sqrt{n} \max_{y \in \mathcal{Y}} \|y\|_2$.

Proof: Define $\text{lip } F(\nu)$, the Lipschitz modulus of a single-valued mapping $F : \mathbb{R}^m \rightarrow \mathbb{R}^n$ at ν [42, Def. 9.1]:

$$\text{lip } F(\nu) = \limsup_{\substack{\nu', \nu'' \rightarrow \nu \\ \nu' \neq \nu''}} \frac{\|F(\nu') - F(\nu'')\|_2}{\|\nu' - \nu''\|_2}. \quad (43)$$

The central step in the proof is to show that $\forall \nu \in \mathbb{R}^n$, $\text{lip } \nabla f^*(\nu) \leq L$, which in turn implies the desired result from [42, Theorem 9.2]. To this end, for each vector $\mathbf{u} = [u_1 \ u_2 \ \dots \ u_n]^T \in \mathbb{R}^n$, define the function $(\mathbf{u} \nabla f^*) : \mathbb{R}^n \rightarrow \mathbb{R}$ by

$$(\mathbf{u} \nabla f^*)(\nu) \triangleq \mathbf{u}^T \nabla f^*(\nu), \quad (44)$$

which is the inner product between \mathbf{u} and $\nabla f^*(\nu)$. Then,

$$\sup_{\|\mathbf{u}\|_2=1} \text{lip } (\mathbf{u} \nabla f^*)(\nu) = \sup_{\|\mathbf{u}\|_2=1} \text{lip} \left(\sum_{i=1}^n u_i \frac{\partial f^*(\nu)}{\partial \nu_i} \right) \quad (45)$$

$$\leq \sup_{\|\mathbf{u}\|_2=1} \sum_{i=1}^n \text{lip} \left(u_i \frac{\partial f^*(\nu)}{\partial \nu_i} \right) \quad (46)$$

$$= \sup_{\|\mathbf{u}\|_2=1} \sum_{i=1}^n |u_i| \text{lip} \frac{\partial f^*(\nu)}{\partial \nu_i} \quad (47)$$

$$\leq \sup_{\|\mathbf{u}\|_2=1} \sum_{i=1}^n \left(|u_i| \max_{y \in \mathcal{Y}} \|y\|_2 \right) \quad (48)$$

$$= \left(\max_{y \in \mathcal{Y}} \|y\|_2 \right) \left(\sup_{\|\mathbf{u}\|_2=1} \|\mathbf{u}\|_1 \right) \quad (49)$$

$$= \sqrt{n} \max_{y \in \mathcal{Y}} \|y\|_2. \quad (50)$$

The equality (45) follows from (44), (46) follows from [42, Exerc. 9.8(b)], (47) follows from [42, Exerc. 9.8(a)], and (48) follows from Lemma 4 and (43) since the scalar-valued function $\partial f^*(\nu)/\partial \nu_i$ is Lipschitz continuous with $\max_{y \in \mathcal{Y}} \|y\|$, (49) follows from trivial rearrangements of terms, and (50) follows directly from the fact that $\sup \|\mathbf{u}\|_1$ is achieved when $\mathbf{u} = [1/\sqrt{n} \ \dots \ 1/\sqrt{n}]^T$. Finally, we note that $\text{lip } \nabla f^*(\nu) = \sup_{\|\mathbf{u}\|_2=1} \text{lip} (\mathbf{u} \nabla f^*)(\nu)$ to conclude the result, cf. [42, Exerc. 9.9]. ■

It is worth noting that the Lipschitzian properties claimed in Proposition 2 *do not* rely on any *strong convexity* properties of f . However, if such properties are imposed on f , Lipschitzian properties of ∇f^* directly follow from the results pertaining to the *dualization of strong convexity*, cf. [42, Theorem 12.60]. The result is summarized in the following Remark.

Remark 6: Suppose the function f_0 is lsc, proper, and strongly convex with constant σ . Then the conjugate function f^* of f is differentiable and its gradient ∇f^* is Lipschitz continuous with constant $M = 1/\sigma$.

Note that the assertions of Proposition 2 are more general than those of Remark 6. This is illustrated by the following example.

Example 5 (Limitations of Remark 6): Let $h_0 : \mathbb{R} \rightarrow \mathbb{R}$ and $l_0 : \mathbb{R} \rightarrow \mathbb{R}$ are defined as $h_0(y) = y^4$ and $l_0(y) = 1 - \sqrt{1 - y^2}$, respectively. Moreover, let $\mathcal{Y} = [-1, 1]$. Note that both h_0 and l_0 and the set \mathcal{Y} fulfill Assumption 1. Let $h = h_0 + \delta y$ and $l = l_0 + \delta y$. Then from Proposition 2, it follows that both ∇h^* and ∇l^* are Lipschitz continuous with the constant 1. However, it is worth pointing out that $\partial^2 h_0(\bar{y})/\partial y^2 = 0$ when $\bar{y} = 0$, and $\partial^2 l_0(\bar{y})/\partial y^2 \rightarrow \infty$ as $\bar{y} \rightarrow \pm 1$. Thus, both h_0 and l_0 are *not strongly convex*. As a result, Remark 6 does not apply in this case.

Following the Lipschitzian properties of f^* [cf. Proposition 2], we establish the Lipschitzian properties of the dual function g as given below.

Corollary 2: Suppose Assumption 1 holds. Then the dual function g is differentiable on \mathbb{R}^m . The gradient ∇g of g is Lipschitz continuous with the constant $G = \|A\|_2^2 L$.

Proof: The identity (8) together with Lemma 3 guarantees the differentiability of g . The same identity together with Proposition 2 guarantees the Lipschitz continuity of ∇g . ■ Note that it can be shown that ∇g is Lipschitz continuous with the constant $\|A\|_2^2 M$ when f_0 is strongly convex, cf. Remark 6.

APPENDIX C

PROOF OF REMARK 4

Recall that $\mathbf{y}^{(k)}$ is the minimizer of the Lagrangian associated to problem (2) with Lagrange multiplier $\lambda^{(k)}$. Then from [42, Prop. 11.3], we have

$$\mathbf{y}^{(k)} = \nabla f^*(\mathbf{A}^T \lambda^{(k)}) \iff \mathbf{A}^T \lambda^{(k)} \in \partial f_0(\mathbf{y}^{(k)}) + \partial \delta_{\mathcal{Y}}(\mathbf{y}^{(k)}).$$

Replacing $\mathbf{y}^{(k)}$ by \bar{y} yields the result. ■

REFERENCES

- [1] Y. Cao, W. Yu, W. Ren, and G. Chen, "An overview of recent progress in the study of distributed multi-agent coordination," *IEEE Trans. Inf. Inform.*, vol. 9, no. 1, pp. 427–438, 2012.

- [2] P. Di Lorenzo, S. Barbarossa, and S. Sardellitti, "Distributed signal processing and optimization based on in-network subspace projections," *IEEE Trans. Signal Process.*, vol. 68, pp. 2061–2076, 2020.
- [3] A. Nedić and J. Liu, "Distributed optimization for control," *Annu. Rev. Control, Robot., Auton. Syst.*, vol. 1, no. 1, pp. 77–103, 2018.
- [4] T. Yang, X. Yi, J. Wu, Y. Yuan, D. Wu, Z. Meng, Y. Hong, H. Wang, Z. Lin, and K. H. Johansson, "A survey of distributed optimization," *Annu. Rev. Control*, vol. 47, pp. 278–305, 2019.
- [5] D. P. Palomar and Y. C. Eldar, *Convex Optimization in Signal Processing and Communications*, Cambridge Univ. Press, NY, 2010.
- [6] H. Hellström, J. M. B. da Silva Jr, V. Fodor, and C. Fischione, "Wireless for machine learning," *Found. and Trends® in Signal Process.*, vol. 15, no. 4, pp. 290–399, 2022.
- [7] B. T. Polyak, *Introduction to Optimization*. NY: Optimization Software, Inc., Publications Division, 1987.
- [8] A. A. Goldstein, "Cauchy's method of minimization," *Numerische Mathematik*, vol. 4, pp. 146–150, 1962.
- [9] L. Armijo, "Minimization of functions having lipschitz continuous first partial derivatives," *Pacific J. Math.*, vol. 16, no. 1, pp. 1–3, 1966.
- [10] A. Beck and M. Teboulle, "Gradient-based algorithms with applications to signal recovery problems," *Convex Optim. in Signal Process. and Commun.*, pp. 42–88, 2009.
- [11] J. Y. Bello Cruz and T. T. A. Nghia, "On the convergence of the forward-backward splitting method with linesearches," *Optim. Methods and Softw.*, vol. 31, no. 6, pp. 1209–1238, 2016.
- [12] A. Asl and M. L. Overton, "Analysis of the gradient method with an Armijo–Wolfe line search on a class of non-smooth convex functions," *Optim. Methods and Softw.*, vol. 35, no. 2, pp. 223–242, 2020.
- [13] S. Khirirat, X. Wang, S. Magnússon, and M. Johansson, "Improved step-size schedules for proximal noisy gradient methods," *IEEE Trans. Signal Process.*, vol. 71, pp. 189–201, 2023.
- [14] T. T. Doan, S. T. Maguluri, and J. Romberg, "On the convergence of distributed subgradient methods under quantization," in *2018 56th Annu. Allerton Conf. Commun., Control, and Comput.*, 2018, pp. 567–574.
- [15] —, "Fast convergence rates of distributed subgradient methods with adaptive quantization," *IEEE Trans. Autom. Control*, vol. 66, no. 5, pp. 2191–2205, 2021.
- [16] N. Z. Shor and M. B. Shchepakina, "Algorithms for the solution of the two-stage problem in stochastic programming," *Cybernetics*, vol. 4, no. 3, pp. 48–50, 1968.
- [17] N. Z. Shor, "The rate of convergence of the generalized gradient descent method," *Cybernetics*, vol. 4, no. 3, pp. 79–80, 1968.
- [18] J.-L. Goffin, "On convergence rates of subgradient optimization methods," *Math. Program.*, vol. 13, pp. 329–347, 1977.
- [19] N. Z. Shor, *Minimization methods for non-differentiable functions*. Springer Science & Business Media, 2012, vol. 3.
- [20] D. Davis, D. Drusvyatskiy, K. J. MacPhee, and C. Paquette, "Subgradient methods for sharp weakly convex functions," *J. Optim. Theory and Appl.*, vol. 179, no. 3, p. 962–982, 2018.
- [21] Z. Zhu, T. Ding, D. Robinson, M. Tsakiris, and R. Vidal, "A linearly convergent method for non-smooth non-convex optimization on the grassmannian with applications to robust subspace and dictionary learning," in *Proc. Advances Neural Inf. Process. Syst.*, vol. 32, 2019.
- [22] N. S. Aybat, A. Fallah, M. Gurbuzbalaban, and A. Ozdaglar, "A universally optimal multistage accelerated stochastic gradient method," in *Proc. Advances Neural Inf. Process. Syst.*, vol. 32, 2019.
- [23] X. Wang, S. Magnússon, and M. Johansson, "On the convergence of step decay step-size for stochastic optimization," in *Proc. Advances Neural Inf. Process. Syst.*, vol. 34, 2021, pp. 14 226–14 238.
- [24] Z. Chen, Z. Yuan, J. Yi, B. Zhou, E. Chen, and T. Yang, "Universal stagewise learning for non-convex problems with convergence on averaged solutions," *arXiv preprint arXiv:1808.06296*, 2019.
- [25] A. Krizhevsky, I. Sutskever, and G. E. Hinton, "Imagenet classification with deep convolutional neural networks," in *Proc. Advances Neural Inf. Process. Syst.*, vol. 25, 2012.
- [26] K. He, X. Zhang, S. Ren, and J. Sun, "Deep residual learning for image recognition," in *Proc. IEEE Conf. Computer Vision and Pattern Recognit.*, 2016, pp. 770–778.
- [27] R. Ge, S. M. Kakade, R. Kidambi, and P. Netrapalli, "The step decay schedule: A near optimal, geometrically decaying learning rate procedure for least squares," in *Proc. Advances Neural Inf. Process. Syst.*, vol. 32, 2019.
- [28] B. T. Polyak, "Minimization of unsmooth functionals," *USSR Comput. Math. and Math. Phys.*, vol. 9, no. 3, pp. 14–29, 1969.
- [29] E. Hazan and S. Kakade, "Revisiting the polyak step size," *arXiv preprint arXiv:1905.00313*, 2022.
- [30] N. Loizou, S. Vaswani, I. H. Laradji, and S. Lacoste-Julien, "Stochastic polyak step-size for sgd: An adaptive learning rate for fast convergence," in *Int. Conf. Artif. Intell. and Statist.* PMLR, 2021, pp. 1306–1314.
- [31] X. Wang, M. Johansson, and T. Zhang, "Generalized polyak step size for first order optimization with momentum," *arXiv preprint arXiv:2305.12939*, 2023.
- [32] J. Barzilai and J. M. Borwein, "Two-point step size gradient methods," *IMA j. Numer. Anal.*, vol. 8, no. 1, pp. 141–148, 1988.
- [33] Y.-H. Dai and L.-Z. Liao, "R-linear convergence of the barzilai and borwein gradient method," *IMA j. Numer. Anal.*, vol. 22, no. 1, pp. 1–10, 2002.
- [34] O. Burdakov, Y.-H. Dai, and N. Huang, "Stabilized barzilai-borwein method," *arXiv preprint arXiv:1907.06409*, 2019.
- [35] Y. Malitsky and K. Mishchenko, "Adaptive gradient descent without descent," in *Proc. 37th Int. Conf. Mach. Learn.*, vol. 119, 2020, pp. 6702–6712. [Online]. Available: <https://proceedings.mlr.press/v119/malitsky20a.html>
- [36] S. Magnússon, H. Shokri-Ghadikolaei, and N. Li, "On maintaining linear convergence of distributed learning and optimization under limited communication," *IEEE Trans. Signal Process.*, vol. 68, pp. 6101–6116, 2020.
- [37] Y. Liu, Y. Sun, and W. Yin, "Decentralized learning with lazy and approximate dual gradients," *IEEE Trans. Signal Process.*, vol. 69, pp. 1362–1377, 2021.
- [38] I. Necoara and V. Nedelcu, "Rate analysis of inexact dual first-order methods application to dual decomposition," *IEEE Trans. Autom. Control*, vol. 59, no. 5, pp. 1232–1243, 2014.
- [39] Y. Su, Z. Wang, M. Cao, M. Jia, and F. Liu, "Convergence analysis of dual decomposition algorithm in distributed optimization: Asynchrony and inexactness," *IEEE Trans. Autom. Control*, vol. 68, no. 8, pp. 4767–4782, 2023.
- [40] S. Boyd, L. Xiao, A. Mutapcic, and J. Mattingley, "Notes on decomposition methods," 2007. [Online]. Available: http://stanford.edu/class/ee364b/lectures/decomposition_notes.pdf
- [41] S. Boyd and L. Vandenberghe, *Convex Optimization*, Cambridge University Press, USA, 2004.
- [42] R. T. Rockafellar and R. J. B. Wets, *Variational Analysis*. Berlin: Springer-Verlag Berlin Heidelberg, 2009.
- [43] M. S. Bazaraa and H. D. Sherali, "On the choice of step size in subgradient optimization," *Eur. J. Oper. Res.*, vol. 7, no. 4, pp. 380–388, 1981.
- [44] P. Bianchi, W. Hachem, and S. Schechtman, "Convergence of constant step stochastic gradient descent for non-smooth non-convex functions," *Set-Valued and Variational Anal.*, vol. 30, pp. 1117–1147, 2022.
- [45] V. S. R. L. V. Singh, S. N. Ravi, and T. Dinh, "Constrained deep learning using conditional gradient and applications in computer vision," *arXiv preprint arXiv:1803.0645*, 2018.
- [46] H. Gouk, E. Frank, B. Pfahringer, and M. J. Cree, "Regularisation of neural networks by enforcing lipschitz continuity," *Mach. Learn.*, vol. 110, pp. 393–416, 2021.
- [47] F. Bach, R. Jenatton, J. Mairal, G. Obozinski *et al.*, "Optimization with sparsity-inducing penalties," *Found. and Trends® in Mach. Learn.*, vol. 4, no. 1, pp. 1–106, 2012.
- [48] G. C. Calafiore and L. El Ghaoui, *Optimization Models*. Cambridge University Press, 2014.
- [49] S. Boyd, N. Parikh, E. Chu, B. Peleato, and J. Eckstein, "Distributed optimization and statistical learning via the alternating direction method of multipliers," *Found. and Trends® in Mach. Learn.*, vol. 3, no. 1, pp. 1–122, 2010.
- [50] J. Chen and A. H. Sayed, "Diffusion adaptation strategies for distributed optimization and learning over networks," *IEEE Trans. Signal Process.*, vol. 60, no. 8, pp. 4289–4305, 2012.
- [51] G. Mancino-Ball, Y. Xu, and J. Chen, "A decentralized primal-dual framework for non-convex smooth consensus optimization," *IEEE Trans. Signal Process.*, vol. 71, pp. 525–538, 2023.
- [52] T. Halsted, O. Shorinwa, J. Yu, and M. Schwager, "A survey of distributed optimization methods for multi-robot systems," 2021. [Online]. Available: <https://arxiv.org/abs/2103.12840>
- [53] T. Hastie, R. Tibshirani, and J. H. Friedman, *The elements of statistical learning: data mining, inference, and prediction*. Springer, 2009.
- [54] I.-C. Yeh, "Real Estate Valuation," UCI Mach. Learn. Repository, 2018, DOI: <https://doi.org/10.24432/CSJ30W>.